CHARACTERIZATION OF A BI-LOBE ASSOCIATED RANGAP IN *TRYPANOSOMA BRUCEI*

SHIMA BAYAT

(M.Sc, University of Tehran)

A THESIS SUBMITTED

FOR THE DEGREE OF DOCTOR OF PHLOSOPHY

DEPARTMENT OF BIOLOGICAL SCIENCES

NATIONAL UNIVERSITY OF SINGAPORE

2013

DECLARATION

I hereby declare that the thesis is my original work and it has been written by me in its entirety. I have duly acknowledged all the sources of information which have been used in this thesis.

This thesis has also not been submitted for any degree in any university previously.

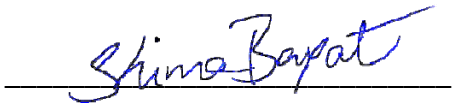

SHIMA BAYAT

14 JANUARY 2013

ACKNOWLEDGEMENTS

I would like to express my deepest gratitude to my dear supervisor Cynthia, for sharing her wisdom and providing me with guidance throughout my graduate career. I am grateful for the opportunity and the freedom she has given me to mature into an independent researcher, and for all the time and effort she spent teaching me to become a better thinker. When it comes to experimental biology, she exudes the kind of optimistic imagination that I needed so desperately when there seemed to be no end, in sight to my project. Her constant encouragement, enthusiasm, and care have also made my time in her lab the most enriching and rewarding.

To my wonderful labmates, past and present. There is no way to thank all these awesome people, for their helpful suggestions, and creative ideas through the course of my study. I thank them for much needed support, encouragement, and most of all, for their friendship, which I would defiantly miss very much.

I would also like to render my appreciation to the National University of Singapore for providing me with monetary support and the opportunity to experience a season of exploration and research.

To my mom and dad, for believing in me and for all their support from far away and for encouraging me to follow my heart and for pursuit my passion during all these years.

To my beloved sister, Elaheh. I love her and thank her for inspiration and her moral support.

And last, but far from least, to my sweetheart, Hossein. He deserves more than just a word of thanks or grateful mention. He deserves a medal for always standing by my

side, for his patience and understanding, and most of all, for taking this incredible journey with me. It has not always been easy, but without you, it would not have been possible. This humble work is dedicated to you…

Shima

13 December 2012

TABLE OF CONTENTS

SUMMARY

Trypanosoma brucei is the causative agent of African trypanosomaisis, commonly referred to as African sleeping sickness in humans. This single-cell parasite contains a single flagellum important for cell movement, division and morphogenesis. Proper flagellum function requires flagellar attachment to the cell body, which is mediated by a specialized flagellum attachment zone (FAZ) complex composed of protein filaments, microtubules, and membranes. A bi-lobed structure locates at the proximal base of the single flagellum and is tightly linked to both the flagellum and the flagellum attachment complex. A leucine-rich repeats (LRR) containing protein TbLRRP1 present on the bilobe is essential for bilobe duplication, FAZ biogenesis, flagellar attachment and cell motility.

To understand the molecular mechanism of TbLRRP1 and to further investigate the function of the bilobe, I used a yeast-two-hybrid screening to search for *T. brucei* proteins interacting with TbLRRP1. Yeast-two-hybrid screening resulted in a number of potential binding candidates, which were then characterized by YFP-tagging in this study. A previously uncharacterized, putative Ran-binding domain containing protein was of particular interest. Detailed characterization of TbLRRP1 interaction with this protein revealed an intriguing role of TbLRRP1 as a Ran GTPase activating protein (RanGAP). TbLRRP1 formed a functional complex with small GTPase Ran and a Ran-binding domain containing protein in *T. brucei* and was required for Ran activation. TbLRRP1 is thus the first Ran GTPase activating protein (RanGAP) found in *T. brucei* and protozoan parasites, and the first RanGAP identified to have a specific role on flagellum function.

LIST OF TABLES

LIST OF FIGURES

LIST OF ABBREVIATIONS

Ade	adenine
APS	ammonium persulfate
aa	amino acids
DAPI	4, 6-diamidino-2-phenylindole
dNTP	deoxyribonucleotide triphosphate
DTT	dithiothreitol
FAZ	flagellum attachment zone
His	Histidine
IPTG	isopropyl β-D-1-thiogalactopyranoside
Kan	Kanamycine
LiAc	Lithium acetate
Leu	Leucine
LB	Luria broth
NPC	Nuclear pore complex
PCR	polymerase chain reaction
RanGAP	Ran GTPase activating protein
RanGEF	Ran guanine nucleotide exchange factor
RNAi	RNA interference
PVDF	polyvinylidene difluoride

SDS-PAGE	sodium dodecyl sulphate polyacrylamide gel electrophoresis
TBST	Tris-buffered saline - Tween 20 buffer
Trp	Tryptophan

CHAPTER 1. Introduction

1.1. An overview of *Trypanosoma brucei*

1.1.1. *T.brucei*: Parasitology, Phylogeny and Ecology

Trypanosoma brucei is the causative agent of African trypanosomaisis, commonly referred to as African sleeping sickness in humans. Sleeping sickness has a devastating impact on human health and prosperity, and is responsible for >0.5 million cases and 70,000 deaths per year (http://www.who.int/en/). The parasite also infects cattle and game animals (where it causes the disease 'nagana'), thereby limiting agricultural development and contributing significantly to poverty in afflicted areas (Simarro et al., 2008). Although its relative importance has paled in comparison with the impact of HIV, the parasite presents a continuous threat of sleeping sickness epidemics because of its persisting animal reservoirs (including the tsetse flies that transmit it). Further inflicted by the breakdown of social and economic infrastructure, sleeping sickness has become the biggest killer in parts of Africa, surpassing HIV/AIDS in provinces of Angola, Congo and Southern Sudan (http://www.who.int/en/). There is currently no vaccine available, and the four existing drug treatments are old (e.g. Suramin, a primary treatment for acute human trypanosomasis, was discovered in 1917 and patented in 1924), difficult to apply in the field and often associated with toxic side effects (Brun et al., 2010).

Trypanosoma brucei spp (comprising *Trypanosoma brucei brucei* and the human infective forms *T. b. rhodesiense* and *T. b. gambiense*) are part of a larger clade of single-celled organisms, collectively referred to as kinetoplastids. The kinetoplastids are likely a monophyletic group, which is related to the euglenoids (Simpson et al., 2006). Three distinct kinetoplastids are known to cause human diseases: *Trypanosoma brucei* spp that cause African sleeping sickness, *Trypanosoma cruzi* that causes Chagas disease, and *Leishmania* spp that cause leishmaniasis. All are parasites of the blood and/or tissues of the human host and are transmitted by arthropod vectors. The most common carrier of *Trypanosoma brucei* is the tsetse fly, which is mostly found in Western and Central Africa, the poorest developing regions in the world. The tsetse fly's habitat varies, depending on the species of the fly and its location, but climate and altitude are determining factors in their distribution (Matthew et al., 2005). *Trypanosoma cruzi* is found in many countries in the Americas, and is carried by insects to animals and humans in much the same way as its African counterpart, although the vectors for *T.cruzi* are bedbugs or "assassin" bugs rather than the tsetse flies. *Trypanosoma cruzi* was once thought to be confined to Brazil and its surrounding area, but recently cases of Chagas disease have been reported as far north as southern North America. Immigrants from Central America and Mexico are thought to be the cause of the disease's migration northward (Reisenman et al., 2010).

1.1.2 *T.brucei*: life cycle

T. brucei spp are parasites with a two-host life cycle; mammals and the tsetse fly (Glossina spp) (Fig 1.1). As such they have to make a series of transitions between at least three major environmental niches; mammalian blood stream, tsetse midgut and tsetse salivary gland. The life cycle starts when the trypanosomes are ingested during a blood meal by the tsetse fly from an infected mammalian host. The parasite proceeds to differentiate into procyclic forms (PCF) in the fly midgut, proliferating and transitioning through several intermediate stages (in strict chronological order) before transforming into the infectious metacyclic stage in the salivary gland of the fly (Roditi and Lehane, 2008; Vickerman et al., 1988). This process necessitates highly coordinated modulation of many basic biological processes (Fenn and Matthews, 2007), suggesting that trypanosomes are not only capable of adapting to rapidly changing environments, they also possess the capacity for rigorously programmed differentiation. Metacyclic, non-proliferating trypanosomes are transferred via insect bite to the dermal tissue of the mammal where they transform into proliferating long slender form. The trypanosomes multiply locally at the site of the bite for a few days before entering the lymphatic system and the blood stream, through which they reach other tissues and organs including the central nervous system (CNS). When cells reach a threshold density in the blood stream, they differentiate into cell cycle arrested short stumpy forms. The occurrence of the cell cycle-arrested short stumpy forms is thought to be important to control the parasitaemia and prevent an early death of the host (Vassella et al., 1997). The

uniform arrest of stumpy form in G1 phase of the cell cycle ensures that the morphological changes that occur upon transmission to the tsetse fly can be coordinated with re-entry into the cell cycle. This is important because correct organelle positioning is crucial for successful completion of the cell cycle of tsetse midgut procyclic forms (Matthews, 2005). During the blood meal of the tsetse fly on an infected mammalian host, short stumpy cells are uptaken by the tsetse vector, starting another transmission cycle. During the entire life cycle, *T. brucei* cells multiply by binary fission (Fig 1.1) and are considered to be exclusively extracellular.

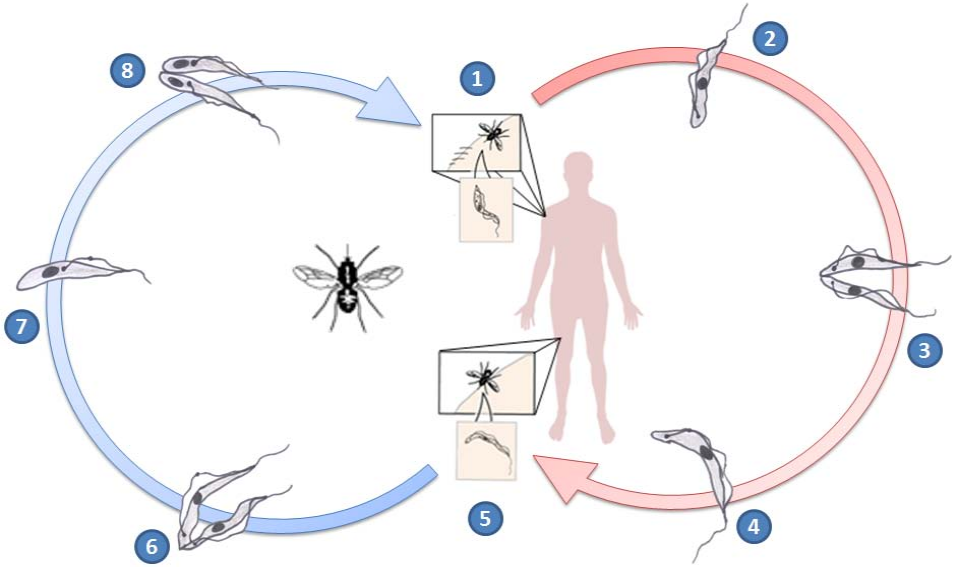

FIGURE 1.1 *T.brucei* life cycle (1) Tsetse fly takes a blood meal (injects metacyclic trypomastigotes). (2) Injected metacyclic trypomastigotes transform into bloodstream trypomastigotes, which are carried to other sites of the body. (3) Trypomastigotes multiply by binary fission in various body fluids e.g., blood, lymph, and spinal fluid (4) Trypomastigotes in blood. (5) Tsetse fly takes a blood meal (bloodstram trypomastigotes are ingested). (6) Bloodstram trypomastigotes transform into procyclic trypomastigotes in tsetse fly midgut. procyclic trypomastigotes multiply by binary fission. (7) Procyclic trypomastigotes leave the midgut and transform into epimastigotes. (8) Epimastigotes multiply in salivary gland, then transform into metacyclic trypomastigotes. (The artwork attained by pencil drawing and Microsoft powerpoint)

1.1.3 *T. brucei* as a model organism

In addition to its relevance to public health and economic development in some of the poorest places in the world, the molecular tools available in trypanosome make it an excellent experimental system in molecular and cellular biology. Studies of trypanosome biology generally consider these protozoan parasites as individual cells in suspension cultures or in animal models of infection. Studies thus far have focused on the proliferative procyclic and bloodstream forms of the parasite, mainly because these stages are readily cultured in vitro (Gull, 1999). As a model system, the single-celled *Trypanosoma brucei* is one of the earliest divergent eukaryotic organisms studied in laboratories. Trypanosomes have followed an evolutionary track distinct from those that are extolled for their conservation of key features, from yeast to human. Some universal cellular pathways operate in Trypanosomes in interestingly different ways, and some biological processes in trypanosomes, though highly conserved, represent unique mechanisms of pathogenicity. Examples are RNA editing and GPI-anchoring of proteins to membranes, which were famously discovered first in the trypanosomes (Low and Finean, 1997, 1998; Low and Zilversmit, 1980; Ikezawa et al., 1976; Taguchi et al., 1980). Development in advanced molecular genetics methods such as heritable and inducible RNA-interference, targeted gene knockouts, stable and inducible overexpression of recombinant proteins allows rapid characterization of protein function (Cross 2001; Kelly et al., 2007; Meissner et al., 2007; Motyka and Englund, 2004). Reverse genetic and post-genomic work has also been

further expedited by the release of the complete genome sequence in 2005 (Aslett et al., 2010; Berriman et al., 2005). Production of large-scale RNAi libraries has provided new tools for the study of potentially interesting genes that have hitherto been overlooked (Alsford et al., 2011; Morris et al., 2002; Burkard et al., 2011).

1.2 *T. brucei* cell biology

1.2.1 Cell morphology and flagellum attachment zone (FAZ)

Although its overall length and shape vary subtly at different points in the life cycle and cell cycle, *T. brucei* is consistently recognizable for its characteristic elongated, flagellate appearance. The motility of the parasite is dependent upon its single flagellum, which has a 9+2 microtubular axoneme with an additional extra-axonemal complex known as the paraflagellar rod (PFR). The flagellum is attached laterally to the cell body in a left-handed helix, beginning from where it exits the cell body via the flagella pocket near the posterior region of the cell along to the anterior (Sherwin and Gull, 2003). This polarized shape, which remains intact throughout much of the various developmental stages, is conferred by the subpellicular corset or cortex. This structure comprises of microtubules crosslinked parallel to each other, forming a microtubule sheet that wraps around the cell body on the interior side of the plasma membrane (Angelopoulos, 1970).

Little is known about the biogenesis of the subpellicular corset, its exact organization and its duplication and inheritance by daughter cells during the binary cell division. Most subpellicular microtubules originate in the anterior

region of the parasite, and terminate at the posterior tip (Sherwin and Gull, 1989a). Using YL1/2, a monoclonal antibody directed to tyrosinated alpha-tubulin, new microtubule synthesis was found in between existing microtubules, suggesting a possible templated model for cortical microtubule duplication (Sherwin and Gull, 1989b). Earlier studies on flagellum protein trafficking suggested a role of flagellum in cell morphogenesis (Kohl et al., 2003), and this is likely mediated by flagellum attachment to the cell body. As mentioned above, the single flagellum is attached laterally to the cell body, via flagellar membrane adhesion proteins (LaCount et al., 2002; Sun et al., 2012) and a mostly intracellular flagellum attachment zone (FAZ). Ultrastructurally, the FAZ is characterized by an electron-dense filament subtending the flagellum and four microtubules in close association with smooth endoplasmic reticulum membranes (Sherwin and Gull, 1989a; Vickerman 1962; Vickerman, 1969). Although little is known about FAZ components and how new FAZ is assembled in proliferating cells, it is increasingly evident that this complex structure plays critical roles in cell division, organelle positioning and cell morphogenesis (LaCount et al., 2002; Morriswood et al., 2009; Shi et al., 2008; Zhou et al., 2010) . Recent work in our lab (Zhou et al., 2012) identified a new FAZ protein CC2D. Depletion of CC2D inhibited new FAZ assembly but not cell division during early RNAi stages, leading to the production of short new daughter cells containing truncated or no FAZ. The length of the FAZ positively correlated to cell length, in both control and CC2D-deficient cells, suggesting a direct role of FAZ in determining cell length, possibly by modulating cortical microtubule synthesis. How FAZ controls

cell length or cortical microtubule assembly remains unknown. It is interesting to note, however, gamma-tubulin has been localized to the posterior region, as well as along the FAZ structure in a previous study (Scott et al., 1997).

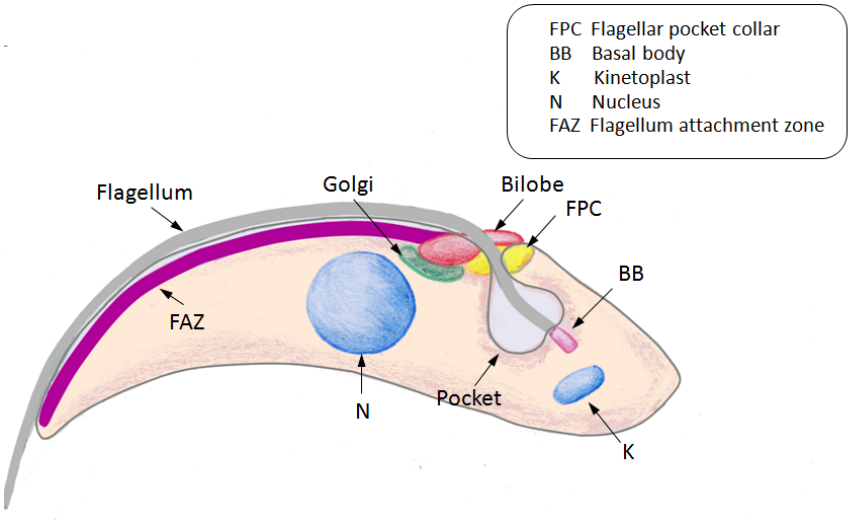

FIGURE 1.2 Major ultrastructural features of procyclic *T. brucei*. Each parasite cell contains a single nucleus (N) and a single kinetoplast (K), a mass of concatenated mitochondrial DNA. The kinetoplast is physically attached to the basal bodies (BB) that seed the growth of the single flagellum (the pro-basal body is not depicted separately here). Upon exit from the cell, the flagellum is attached to the cell body via the flagellum attachment zone (FAZ). A single Golgi apparatus is present at the proximal base of the FAZ, adjacent to the flagellar pocket where endocytosis and exocytosis take place and a bilobe structure in close association with flagellar pocket collar (FPC) that constricts the flagellar pocket membrane around the flagellum. (The artwork attained by pencil drawing)

1.2.2 *T. brucei* cell cycle

The high degree of structural organization of *T. brucei* greatly facilitates microscopic analysis of cell cycle and organelle inheritance (Fig 1.2). The cell cycle initiates with the elongation and maturation of the pro-basal body and the nucleation of a new flagellum. The Golgi situated between the nucleus and the

flagellar pocket, is the next to undergo duplication. Kinetoplast S phase initiates before the onset of nuclear S phase and is considerably shorter. Early in G2 phase of the nuclear cycle, basal bodies separate in a microtubule mediated process, resulting in the separation of the kinetoplasts) that are coupled to the basal bodies via the tripartite attachment complex (TAC) (Robinson et al., 1991; Ogbadoyi et al., 2003). Mitosis occurs with an intranuclear spindle without the disruption of the nuclear envelope. The actual mechanism of chromosome segregation remains unknown, and the number of chromosomes exceeds the number of kinetochores (Ogbadoyi et al., 2000). The cell cycle is completed by cytokinesis with the formation of the cleavage furrow along the entire longitudinal axis of the dividing trypanosome.

Several unusual features have been observed for trypanosome cell cycle (Hammarton et al., 2007). The first is the strict regulation of organelle positioning during division. Thus, the kinetoplast-nucleus, and kinetoplast-posterior dimensions are fixed during the cell cycle of the procyclic form, cell growth at the posterior end occurring between the segregating basal bodies and being maintained throughout S, G2 and M phase (Robinson et al., 1995). The second is the observation that cytokinesis is not dependent upon the completion of nuclear mitosis. Disruption of the mitotic spindle by drugs or genetic perturbation of trypanosome cyclin-dependent kinases (CDKs) generates zoids that has a mitochondrial genome but no nucleus (Ploubidou et al., 1999, Hammarton et al., 2003; Li and Wang, 2003). Cells are classified as 1K1N, 2K1N or 2K2N cells;

according to the number of nuclei (N) or kinetoplasts (K) each cell contains (Fig 1.3). 1K2N cells do not normally exist since the kinetoplasts always segregate before the nucleus divides.

Interestingly, organelle positioning and nuclear division have both been linked to FAZ functions, although the detailed mechanisms remain unclear (Absalon et al., 2007, 2008; Vaughan et al., 2008). New FAZ assembly occurs even prior to the basal body duplications (LaComble et al., 2010; Gheiratmand et al., 2013). New FAZ elongates co-ordinatedly with the new flagellum (Kohl et al., 1999), posterior to the old structures. This co-ordinated elongation coincides with synthesis of new subpellicular microtubules, increase in cell length and the segregation of the duplicated organelles (Fig 1.3). The critical position of the FAZ also suggests a role of this structure in cell division (Robinson et al., 1995).

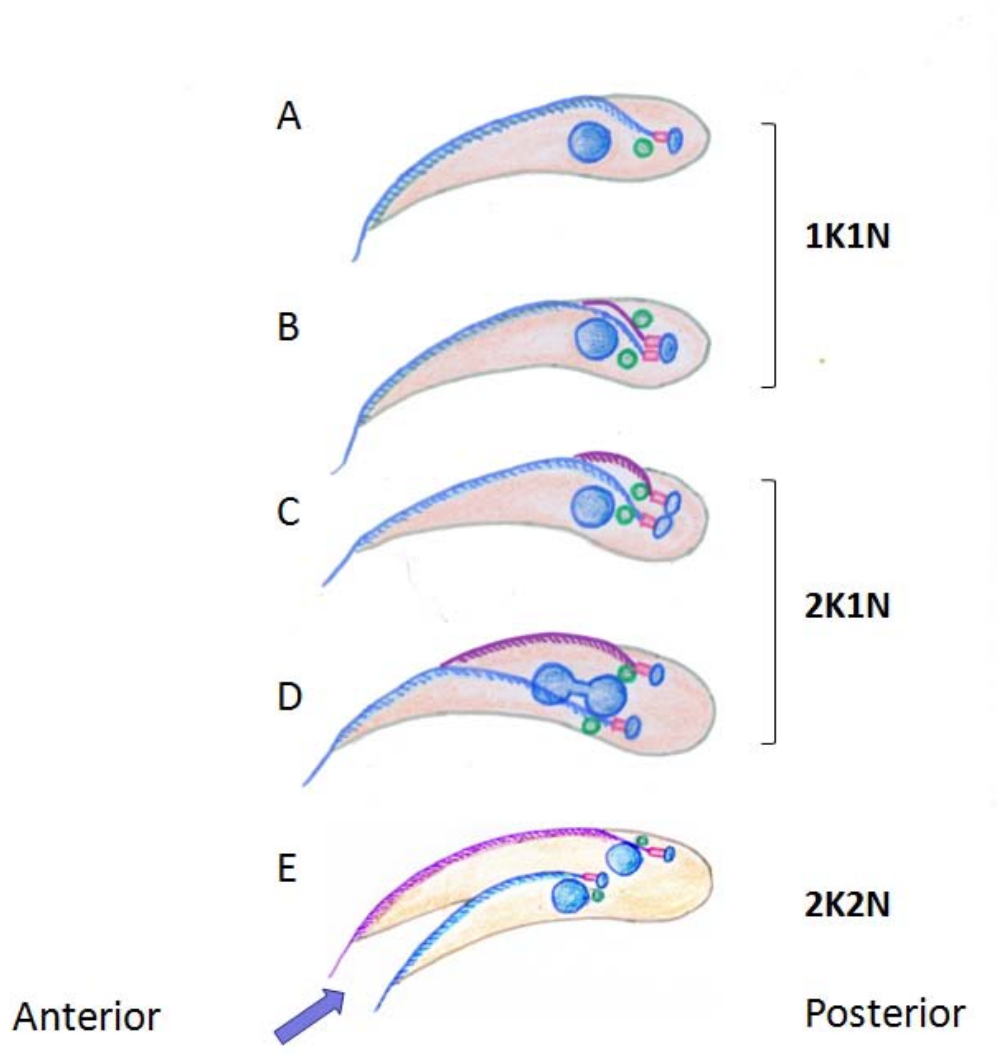

FIGURE 1.3 Cartoon presentation of the major cell cycle stages of *T.brucei.* (A) A single copy of the major organelles (nucleus, kinetoplast, basal body and the Golgi apparatus) are present in an interphase cell. The single flagellum is tethered to the cell body via the FAZ structure. (B-E) As the cell undergoes cell division, the organelles duplicate and segregate in strict chronological and temporal order, which culminates in cytokinesis. This allows parasite cell cycle stages to also be categorized according to the division and segregation state of the nucleus and kinetoplast (1K1N, 2K1N, 2K2N). Small blue circle, kinetoplast; green circle, Golgi; pink rectangle, basal bodies; large blue circle, nucleus. The older, existing flagellum is marked in blue while the new flagellum is marked in purple. Both the new and old FAZ structures are represented by a series of lines undergirding the flagella. (The artwork attained by pencil drawing)

1.3 The bi-lobed structure

Whereas little is known about how new FAZ assembly is regulated during the cell cycle, a bi-lobed structure, initially identified to be important for Golgi and ER exit site duplication (He et al., 2005), seems to play a pertinent role in FAZ assembly.

1.3.1 Bilobe; an enigmatic feature of *T.brucei* with unclear function

The bilobe structure of *T.brucei* was serendipitously discovered by immunofluorescence using a pan-centrin monoclonal antibody 20H5 with a defined localization adjacent to the Golgi in the vicinity of the flagellar exit point and was originally proposed to mediate biogenesis of the Golgi complex (He et al., 2005). It was shown that early in the cell cycle, the old Golgi was adjacent to one lobe of the bilobe structure, whereas the new Golgi was later assembled at the other, more posterior lobe. This ensures that each daughter cell inherits one bilobe and one Golgi. During segregation of organelles and structures prior to cytokinesis, the bilobe structure itself duplicates and one Golgi remains associated with each bilobe structure.

1.3.2 Morphology of the bilobe structure

Ultrastructural studies using electron microscopy has led to a deep understanding of different cellular components in different types of trypanosomes for over 50

years. Using electron tomography, the first integrated view of the flagellar pocket and basal body of the *Trypanosoma brucei* was obtained (Lacomble et al., 2009). However, this study was unable to perceive a specific separate cytoskeletal structure corresponding to bilobe in this area. The 3D description does suggest that the neck region is a good candidate for a cytoskeletal structure that defines not only the position of the single Golgi but also the flagellar exit point and flagellar pocket collar. Recent biochemical studies on detergent-extracted flagellum suggest a tight link between the FAZ filament and the bilobe structure (Morriswood et al., 2009; Zhou et al., 2010). The centrally located bilobe overlaps with the posterior tip of the FAZ and duplication of the bilobe is immediately followed by formation of a new FAZ. Inhibition of bilobe duplication also inhibits new FAZ formation (Shi et al., 2008; de Graffenried et al., 2008; Zhou et al., 2010).

A more recent investigation of the bilobe structure takes advantage of its strong association with the flagellum (Esson et al., 2012). By focusing on TbMORN1, which is the first protein localized exclusively to the bilobe (Morriswood et al., 2009), this group has carried out an ultrastructural analysis of the bilobe on detergent-extracted flagella that are negatively stained. This approach provided a clear view of the flagellum-associated bilobe and other structures including the flagellar pocket collar (FPC), a ring structure delimiting the flagellar exit site from the cell body. At the EM level, TbMORN1 labelled a fishhook-shaped pattern at the base of detergent-extracted flagellum, colocalizing precisely with

TbLRRP1, another exclusive bilobe marker. However, TbCentrin4 appeared to localize to a different domain of the bilobe, suggesting the structural complexity of the bilobe structure.

1.3.3 Bilobe protein components

Up to now, four proteins have been shown to localize stably to the bilobe: **TbCentrin2**, **TbCentrin4**, **TbMORN1**, and **TbLRRP1**. Centrins are highly conserved Ca^{2+} binding proteins which are readily identified on microtubule organizing centers of eukaryotes. In *T. brucei,* TbCentrin2 and TbCentrin4 are both additionally present at the basal bodies that nucleate flagellum microtubule axoneme (He et al., 2005; Shi et al., 2008). However, RNAi- mediated ablation revealed different cellular functions for TbCentrin2 and TbCentrin4 during the cell cycle. At the early stage of TbCentrin2 depletion, basal bodies and kinetoplast division were inhibited and large multinucleated cells accumulated because of the inhibition of cytokinesis. Golgi duplication was also inhibited by TbCentrin2 depletion (He et al., 2005). Conversely, basal bodies and Golgi duplication were not affected by TbCentrin4 depletion. However, the coordination between nucleus division and cytokinesis may be disturbed by TbCentrin4-RNAi (Shi et al., 2008). TbMORN1 (a membrane occupation and recognition nexus repeat protein), was the first protein to be identified that was localized exclusively to the bilobe (Morriswood et al., 2009). This study has shown that the bilobe co-purifies with the trypanosome flagellum and is therefore intimately associated with the flagellar

cytoskeleton. They have also shown that the TbMORN1 depletion had a moderate inhibitory effect on cell growth in procyclic but was lethal in the bloodstream stage parasite.

Polo-Like Kinases (PLKs) are conserved migratory proteins that are known to regulate multiple events during cell division among the Eukaryotes. In mammalian cells PLK1 plays important roles in centriole separation, chromosome congression and cytokinesis (Barr et al., 2004; Archambault and Glover, 2009). This protein is initially found on the centrosome, then migrates to spindle poles and the kinetochores following the breakdown of the nuclear envelope, and finally localizes to the central spindle and midbody prior to cytokinesis (Golsteyn et al., 1994; Golsteyn et al., 1995). Depletion of PLK1, leads to defects in spindle pole formation and chromosome congression (Peters et al., 2006).

T. brucei contains a single PLK homologue (TbPLK), that had been implicated in cytokinesis (Kumar and Wang, 2006; Hammarton et al., 2007) and also in the process of bilobe duplication (de Graffenried et al., 2008). Given the role played by PLK in Golgi biogenesis in mammalian cells, the possible involvement of PLK in Golgi biogenesis in *T.brucei* has been investigated by de Graffenried and co workers in 2008 and they showed that the TbPLK plays a key role in the biogenesis of the bilobe, which in turn affects the biogenesis of the Golgi. In contrast to mammalian PLKs, TbPLK does not appear to play a role in mitosis. In a more recent study (Ikeda et al., 2012), the movement of TbPLK1 throughout the cell cycle is examined and the effect of its depletion on several flagellum-

associated cytoskeletal structures is determined. TbPLK initially to the MtQ, then the basal bodies, subsequently progresses to the FPC, bilobe, FC and, finally, to the growing tip of the new FAZ. This pattern closely matches the order in which these structures duplicate, suggesting that TbPLK triggers the replication or inheritance of these cytoskeletal elements.

1.4 TbLRRP1

1.4.1 Identification and structural domain organization

TbLRRP1 was first characterized in the flagellar proteome and was named TbHERTS (Broadhead et al., 2006). A later comparative proteomics study found TbLRRP1 localizing exclusively to the bilobe (Zhou et al., 2010). The 713-amino acid TbLRRP1 comprises of an LRR-containing domain followed with a C-terminal coiled-coil region (Fig 1.4A). Both coiled coil and LRR motifs are widely present in organisms from prokaryotes to eukaryotes. In general, coiled-coils are implicated in protein oligomerization (Burkhard et al., 2001) and LRRs mediate protein-protein interactions (Kobe et al., 2001). Orthologs of TbLRRP1 were found in *Trypanosoma cruzi* and *Leishmania major* (Fig 1.4B). Proteins with little sequence homology but similar domain organizations have been identified and found associated with centrosomes or basal bodies in other flagellated/ciliated organisms, eg. Vfl1 in Chlamydomonas and CLERC in humans. Deficiency in these proteins leads to flagellum biogenesis and mitotic spindle pole defects (Muto et al., 2010). However, the LRRs in Vfl1 and CLERC

are SDS22-like; whereas the LRR in TbLRRP1 belongs to the RI-like subfamily, which has been found in ribonuclease inhibitors and yeast rna1, a RanGAP (Hillig et al., 1999), suggesting perhaps functional difference between these LRRs.

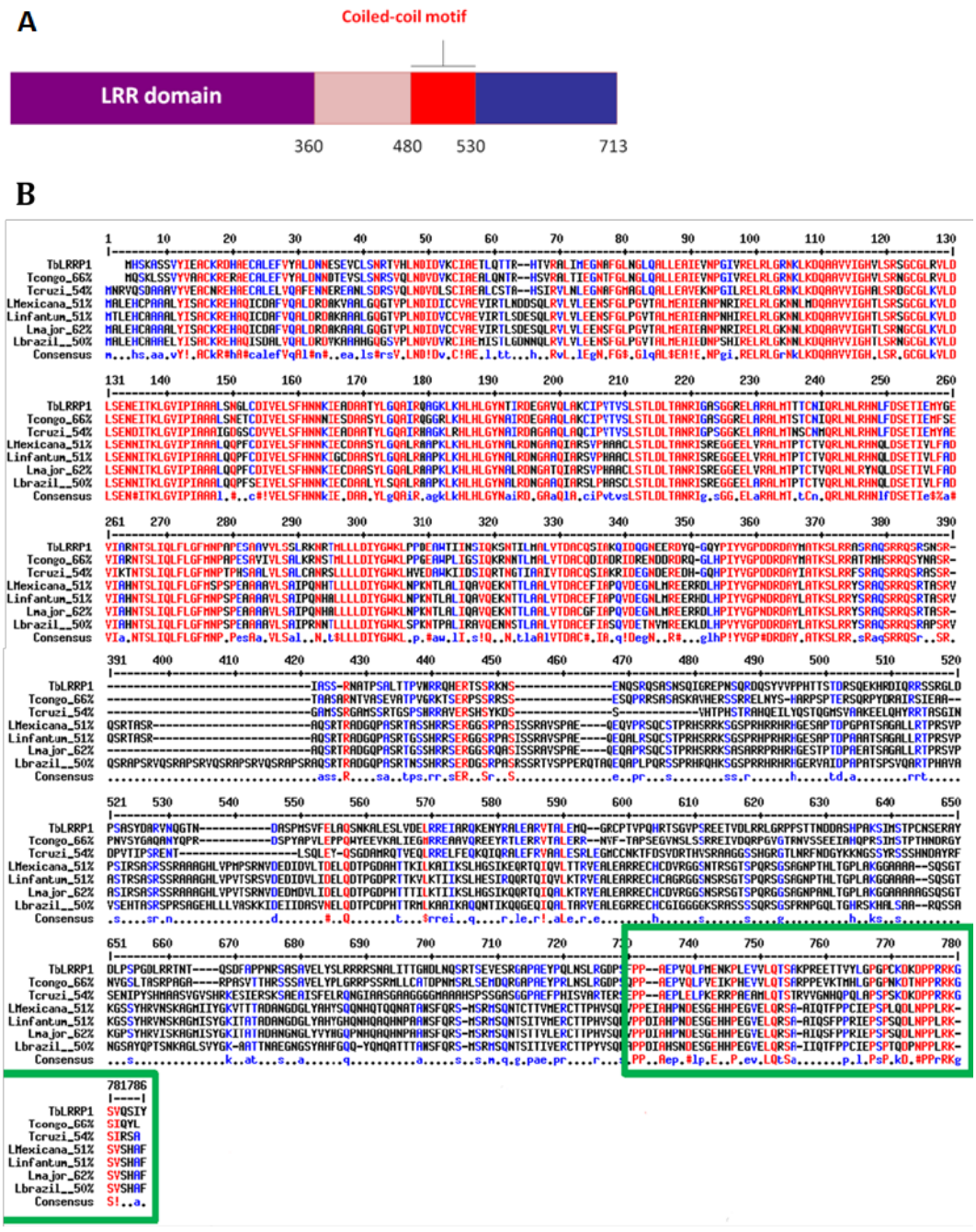

FIGURE 1.4 The domain organization of TbLRRP1. (A) The diagram represents the functional domains annotated for TbLRRP1 using SMART program. TbLRRP1 contains a leucine-rich repeats-containing (LRR) domain in its N-terminal region and a coiled-coil motif in its C-terminal region. Numbers indicate amino acid residues. (B) TbLRRP1 sequence alignment along with the orthologs in some other members of Trypanosomatids. The 400 first residues of TbLRRP1 are mostly conserved and form the

LRR motif. The region represented in green box is a conserved C-terminal sequence.

1.4.2 Cellular localization

Localization of TbLRRP1 to the Golgi-associated bilobe structure has been examined by overexpression of the protein as YFP-fusion and confirmed by specific mouse monoclonal anti-TbLRRP1 antibodies (Zhou et al., 2010). Like TbMORN1, TbLRRP1 was localized exclusively to the bilobe structure, but not at the basal bodies, which are also stained by anti-TbCentrin4, TbCentrin2 and TbCentrin4. This observation was confirmed by immunoEM of both isolated flagellum preparations and detergent-extracted cells (Ikeda et al., 2012).

1.4.3 The functional analysis

Initially, the function of TbLRRP1 was evaluated using tetracycline-inducible RNA interference (RNAi) (Broadhead et al., 2006). They reported an inhibitory effect on parasite motility upon TbLRRP1 depletion. This observation was confirmed by later work (Zhou et al., 2010). Furthermore, the effects of TbLRRP1-RNAi on organelle duplication and cell division were also evaluated. Cell duplication slowed and then stopped ~72-hour post RNAi. Whereas bilobe and Golgi duplication were both inhibited, basal body and kinetoplast duplicated normally, but their segregation was defective, leading to the appearance of detached new flagella and a concomitant reduction in new FAZ structure. With an exception of TbMORN1, depletion of the bilobe proteins in procyclic *T. brucei* has a common effect on organelle duplication and / or cell division. Most

interestingly, the Golgi, FPC and FAZ have all been shown to be adjacent or partially overlapped with the bilobe structure (He et al., 2005; Shi et al., 2008; Morriswood et al., 2009; Zhou et al., 2010). These observations emphasized the biochemical and structural complexity of the bilobe, its extensive association with adjacent organelles and structures, and its critical role in co-ordinating organelle duplication, organelle segregation and cell division events. But how does the bilobe work?

1.5 The purpose of this study

T. brucei LRRP1 was identified as a bilobe component in a comparative proteomics screening for flagellum associated proteins (Zhou et al., 2010). As the only exclusive bilobe protein essential for cell survival, TbLRRP1 provided a specific marker to investigate bilobe association with other organelles (Gheiratmand et al., 2013), and a useful tool to understand bilobe function. The cellular function of TbLRRP1 in organelle duplication/segregation, cell motility and cell division has been thoroughly analyzed in previous studies (Zhou et al., 2010), but its molecular mechanism is yet to be understood.

To understand the molecular mechanism of TbLRRP1 and to further investigate the function of the bilobe, I used a yeast-two-hybrid screening to search for *T. brucei* proteins interacting with TbLRRP1. Yeast-two-hybrid screening resulted in a number of potential binding candidates, which were then characterized by

YFP-tagging. A previously uncharacterized, putative Ran-binding domain containing protein was of particular interest. Detailed characterization of TbLRRP1 interaction with this protein revealed an intriguing role of TbLRRP1 as a putative Ran GTPase activating protein (RanGAP).

CHAPTER 2 Materials and Methods

2.1 Yeast-Two-Hybrid screening

2.1.1 cDNA library construction

Procyclic *T. brucei* (YTat1.1) cDNA library was generated using a Matchmaker™ Library Construction kit following manufacturer's instructions (Clontech). First, *T.brucei* mRNA was isolated with Fast Track® MAG Maxi mRNA isolation kit (Invitrogen, USA). 1-2µl purified mRNA (1µg) and 1µl CDSIII primer were mixed using appropriate amount of deionized H_2O to adjust the total volume to 4µl. The mixture were incubated at 72°C for 2min and rapidly cooled on ice for 2 min. After cooling, 2µl 5X-First-Strand Buffer, 1µl 2mM DTT, 1µl dNTPs (10mM), and 1µl MMLV Reverse Transcriptase were added into the tube, mixed and then incubated at 42°C for 10min before addition of 1µl SMART III Oligonucleotide, followed by incubation at 42°C for 1 hour. Reaction was then terminated at 75°C for 10 min. After the temperature of contents in the tube reached room temperature, template RNA was degraded by adding RNase H (1µl) at 37°C for 20min. Double stranded cDNA was amplified in a 100µl reaction including 2µl first-strand cDNA synthesized from previous step, 70µl deionized H_2O, 10µl 10XAdvantage 2 PCR Buffer, 2µl 10mM dNTP mix, 2µl 5' PCR primer, 2µl 3' PCR primer, 10µl 10X GC-Melt Solution, 2µl 50XAdvantage 2 Polymerase Mix. After PCR amplification, double stranded cDNA was purified with CHROMA SPIN TE-400 Column (Clontech) according to instructions. Double-strand cDNA was then co-transfected with linearized pGADT7-Rec

plasmid into yeast stain AH109, creating the activation domain library that was used as prey (Zhang, 2012).

2.1.2 Bait plasmid construction

In order to generate the bait construct for yeast-two-hybrid assay, either the LRR domain (1-349 aa) or the coiled-coil domain (480-530 aa) of TbLRRP1 was cloned into the pGBKT7 vector (Clontech). The desired fragments were inserted into the multi-cloning site of the pGBKT7 vector using EcoRI and BamHI restriction sites, allowing in-frame fusion to the Gal4-DNA binding domain in the vector. The bait constructs were then tested for transcriptional auto-activity and toxicity. The growth rate of the cells transformed with the bait-plasmids (pGBKT7-LRR and pGBKT7-Coiled-coil) was about three-times slower than those transformed with the empty pGBKT7 plasmid, suggesting that expression of the bait proteins was toxic to yeast cells. Because in some cases strains that do not grow well in liquid culture can grow reasonably well on agar plates, yeast colonies were resuspended in 1 ml of SD/-Trp, and the cell suspension was spread on five 100-mm SD/-Trp plates, which were incubated at 30°C until the colonies were confluent. All colonies from each plate were resuspended in a total of 5ml of 0.5X YPDA, which were used further in the normal mating procedure.

2.1.3 Preparation of yeast competent cells and small-scale yeast transformation

Yeast cells (Y187 or AH109) were streaked on YPDA agar (Clontech) plate and incubated at 30°C for 2-4 days to allow growth of single colonies. A single colony (2-3mm in diameter) was then inoculated into 1.5 ml YPDA medium and incubated at 30°C for 16-20hrs on shaker at 300rpm. The cells from 1 ml of the culture were harvested at 12,000 rpm for 1min and resuspended in a mixture of 80µl 50% PEG-3550, 10µl 1M DTT and 5µl 4M LiAC. For transformation, 500ng plasmid DNA and denatured carrier DNA (5µl 10µg/ml stock) were mixed in a separate 1.5 ml microcentrifuge tube and incubated on ice for 10 min. Competent cells were then added to the DNA mixture and incubated at 45°C for 30 min. Thorough mixing was performed by vortexing every 10 min during the incubation. Cells were then spread on to plate containing SD/-Trp medium.

2.1.4 Yeast mating

1ml aliquot of the *T. brucei* cDNA library in AH109 and 5ml ($\geq 1\times10^9$ cells/ml) of Y187 transformed with bait construct were combined in a sterile 2L flask containing 40ml 2X YPDA/Kan (50µg/ml). The flask was then incubated at 30°C for 20-24hrs with gentle swirling (30-50rpm). After mating, the mixture was centrifuged at 1,000xg for 10 min. Cell pellet was resuspended in 10ml 0.5XYPDA/Kan (50µg/ml). To determine the mating efficiency, 100µl of a 1:10000, 1:1000, 1:100 and 1:10 dilutions of the mating mixture was spread on

three different selective plates (SD/-Trp, SD/-Leu, SD/-Trp/-Leu). Next, the viable colony forming unit (cfu)/ml of the two mating strains was compared. In this library screening, the AH109 strain had lower cfu on SD/-Trp (0.696) compare to Y187 strain (cfu=1.220) on SD/-Leu and therefore AH109 was the limiting partner to ensure that the maximum number of library cells find a mating partner. (cfu)/ml on SD/-Leu/-Trp been calculated as viability of diploids. By dividing the cfu/ml of diploids by cfu/ml of limiting parner, the mating efficiency calculated as 28.67%. Cell suspension was then spread on selective medium SD/-Trp/-Leu/-His/-ade on agar plates. After 5 days of incubation at 30°C, diploids expressing interacting proteins appeared on the plates. To eliminate the most common class of false-positive colonies, Ade^+/His^+ colonies were streaked out on fresh SD/-Ade/-His/-Leu/-Trp/X-α-Gal master plates and incubated for 4-5 days at 30°C to test Ade^+/His^+ colonies for the third reporter; *MEL1*. Positive blue colonies were then further analyzed by PCR colony screening. Glycerol stock cultures of potential positive colonies were frozen at -80°C for long-term storage.

2.1.5 Identify the cDNA inserts from positive colonies

To identify the genes (and thus proteins) responsible for the positive two-hybrid interactions, the cDNA inserts were rescued by PCR colony-screening using Matchmaker AD LD-insert screening amplimer set (Clontech). The PCR products were then analyzed by gel electrophoresis and excised from the gel for DNA purification and sequencing. The DNA sequences were blasted against *T. brucei* genomics sequences in the tritryp databases (tritryp.org).

2.2 Molecular cloning

Full-length coding sequences of the putative binding candidates identified from the yeast-two-hybrid screening were then amplified via polymerase chain reaction (PCR). Standard PCR was generally performed in 50µl reaction volume, using purified *T. brucei* genomic DNA as template. All reactions were carried out on DNA Engine® Peltier Thermal Cycler or My Cycler™ Thermal Cycler (Bio-Rad, USA). PCR products were fractionated by agarose gel electrophoresis (1%-2%, run at 10V/cm). Desired fragments were excised for purification using QIAquick PCR Purification Kit (QIAGEN). Purified DNA fragments and their designated plasmids vectors were subsequently digested with suitable restriction enzymes, followed with ligation overnight at 16°C at a molar ratio of 1:3 (vector: insert). Transformation was performed by heat shock into competent E. coli TOP10 cells. Plasmids harvested from single colonies were then checked for the inserts by restriction digest and/or DNA sequencing.

2.3 *T.brucei* methods

2.3.1 Culture of procyclic *T. brucei*

All experiments described in this thesis were performed on procyclic cell lines - YTat1.1 (*T. brucei rhodesiense)* (Ruben et al., 1983), and 29.13 (*T. brucei brucei*) that allows tetracycline-inducible expression (Wirtz et al., 1999). YTat1.1 cells were cultivated at 28°C in Cunningham's medium supplemented with 15% heat-

inactivated fetal bovine serum (Hyclone). 29.13 cells were maintained at 28°C in Cunningham medium containing 15% heat-inactivated, tetracycline-free fetal bovine serum (Clontech) in the presence of 15μg/ml G418 and 50μg/ml hygromycin. The cell density was maintained between 2×10^6 and 2×10^7 cells/ml by dilutions.

2.3.2 Transient and stable transfection of procyclic *T.brucei*

Plasmids were transfected either transiently or stably by electroporation into parasite procyclic cells. 30-50μg of plasmid was typically used in a transient transfection, while a stable transfection required at least 15μg of linearlized plasmid. To precipitate DNA, plasmid was mixed with 2.5 volume 100% ethanol and 1/10 volume 3M sodium acetate (pH5.2). DNA was precipitated by centrifugation at 13,000 rpm for 10 min at 4°C. DNA pellet was washed twice with 70% ethanol, air dried, and dissolved completely in 500μl cytomix (25mM Hepes, 120mM KCl, 0.15mM $CaCl_2$, 10mM K_2HPO_4, 2mM EGTA, 5mM $MgCl_2$, adjusted with KOH to pH7.6).

Approximately $5x10^7$ log-phase cells were harvested by centrifugation at 3,000 rpm for 7min, washed once with 5ml cytomix, resuspended in 500μl cytomix and mixed with plasmid DNA. The mixture was then transferred to a 4mm-gap cuvette and electroporated twice using a BioRad Gene Pulser (1500 V, 25 μF, ∞ Ω), with 10 seconds in between pulses. Transiently transfected cells were checked for ectopic gene expression between 16-48 hours post transfection, while cells

undergoing stable transfection were typically cloned by limiting dilutions and subjected to antibiotic selection 8-12 hours post transfection.

2.3.3 Clonal selection of stable transformants by limiting dilution

In order to obtain clonal cell lines of stably-transfected cells, parasite cultures were serially diluted in a 96-well microtiter plate such that the parasites were eventually cultured at dilutions below one cell per well (Rosario, 1981). To accomplish this, parasite cultures growing in mid log-phase were diluted two fold in each subsequent column of wells, resulting in a maximum dilution of 2^{11} times the original culture concentration. Appropriate antibiotics was then added using multichannel pipets into each well for selection. Plates were sealed with parafilm and incubated at 28°C, 5% CO2 for approximately 10-15 days until clonal cultures were obtained.

2.4 RNA interference (RNAi)

Specific RNAi target to a certain gene is selected by RNAit (http://trypanofan.path.cam.ac.uk/software/RNAit.html) (Redmond et al., 2003). The DNA fragment corresponding to the target region was cloned into pZJM and/or p2T7 vector in between the XbaI sites. RNAi constructs were then linearized with NotI and transfected into 29.13 cells. Stable, clonal transfectants were obtained by limiting dilution and antibiotics selection. Production of double-

stranded RNA in these cells was induced by tetracycline (10μg/ml). To evaluate RNAi efficiency, *T. brucei* cultures were sampled every 24 hours to monitor cell growth by cell counting, specific protein depletion by immunoblots and cellular phenotypes by light microscopy.

2.5 Immunofluoresence microscopy

Log-phase *T.brucei* cells were harvested by centrigugation at 4600 rpm for 1 min, washed once with PBS (137mM sodium chloride, 2.7mM potassium chloride, 7mM disodium hydrogen phosphate, 3mM sodium dihydrogen phosphate, pH7.4), spread on glass coverslips and allowed the cells to attach for 30 min. Cells were then either permeabilized and fixed in cold methanol at -20°C for 7-10 minutes or fixed in 4% paraformaldehyde (PFA) followed by permeabilization with 0.2% Triton X-100 in PBS. Whenever extraction was needed, cells were treated with either 1% Triton X-100 or 1% Nonidet P40 in PBS 15 min at room temperature, then fixed with 4% PFA for 20 minutes at 4°C. Fixed cells on coverslip were blocked with 3% BSA in PBS for 1 hour to prevent non-specific antibody binding. Cells were then incubated with primary antibody followed with appropriate secondary antibody and counter-stained with 2μg/ml 4, 6-diamidino-2-phenylindole (DAPI) for 20 minutes. After several washes with PBS, the cells were rinsed with milli-Q water and the coverslips were mounted with fluorescence mounting medium (SouthernBiotech Fluoromount-GTM) and air dried before observation. All primary antibodies used in this study and their relevant dilutions are listed in

Table 2. All fluorescein-conjugated secondary antibodies (Sigma) were used at 1:2000 dilution. All samples were observed with a Zeiss inverted microscope (model Axio Observer Z1) equipped with a CCD camera (model CoolSNAP HQ2, Photometrics). Images were processed with Adobe Photoshop CS5.

2.6 Immunoblotting analyses

Parasite cells were washed with PBS, lysed by boiling at 100°C for 5 minutes in the presence of SDS Loading Buffer (3x stock: 150 mM Tris-HCl, pH6.8, 6% SDS, 30% glycerol, 2.5% 2-mercaptoethanol, 0.06% Bromophenol Blue). Denatured cell lysates were resolved by 12% acrylamide gel, electrophoresed at 120V for 1.5-2 hours. Proteins were then electrophoretically transferred onto a methanol-activated PVDF membrane for an hour at 70V. The membranes were blocked with 5% milk in TBST (0.1% Tween-20,10mM Tris-HCl, 150mM NaCl, pH7.6) for an hour prior to incubation with appropriate primary antibodies and horseradish peroxidase-conjugated secondary antibodies. After extensive washes in TBST, the blots were incubated with SuperSignal® West Dura Extended Duration Substrate solution (Thermo Scientific), and imaged using a chemoilluminescence detector (model ImageQuant LAS 4000, GE Healthcare). Should there be a need to re-probe the membrane with different antibodies, the membrane was stripped with stripping buffer (2% SDS, 62.5 mM Tris-HCl, pH6.8, 100 mM 2-mercaptoethanol) for 30 minutes at 60°C, followed by brief

washes with TBST. Membranes were then blocked again with 5% milk in TBST before incubation with the desired antibodies.

2.7 Coomassie Blue staining

After electrophoresis, SDS-PAGE gels were transferred to staining solution containing 0.1% Coomassie Brilliant Blue R250, 10% acidic acid and 40% ethanol. Staining was performed for 45min to overnight with gentle shaking on a platform shaker. The gel was then distained with solution containing 10% acidic acid and 40% ethanol, with multiple changes of the distaining solution until desired intensity and contrast.

2.8 Expression and purification of recombinant proteins in *E. coli*

Single colony of transformed BL21 cells was inoculated into LB medium containing appropriate antibiotic and cultured overnight at 37°C with shaking. The overnight culture was diluted with fresh cell culture medium (1:50) and cultured at 37°C until the OD600 reached 0.6-0.8. Isopropyl-beta-D-thiogalactoside (IPTG) was then added into cell culture to the final concentration of 100μM to induce expression of recombinant protein. Induction was typically performed at 37°C with shaking for 4 hours. Cells were subsequently harvested by centrifugation at 4000rpm at 4°C for 20min. In case protein purification does not proceed immediately after cell harvest, the cell pellet can be snap frozen in liquid nitrogen and stored at -80°C until use.

For GST-fusion protein purification, the bacterial cells were resuspended in ice-cold PBS supplemented with 2mM EDTA (pH8.0), protease inhibitors (Roche; 1 tablet in each 50ml PBS) and 100µg/ml lysozyme. The cells were stored on ice for 30min and then homogenized by sonication until the lysate became clear. Triton X-100 (1% final) and DNaseI (1U/ml final) were then added to the cell lysates, which were incubated with gentle rotation at 4°C for 2 hours. After complete cell lysis, the lysates were centrifuged at 12,000rpm for 20min at 4°C. Cleared supernatant containing soluble GST-tagged proteins was incubated with gluthatione sepharose beads (GE,Healthcare,UK) at 4°C with gentle rotation for 1-2 hours to allow binding. The sepharose beads were then washed 3 times with 10ml PBS containing 1% Triton-X-100 and protease inhibitors, followed by 3 more times with PBS only. After the last PBS wash, beads were resuspended in 10ml PBS and loaded to a chromatography column. GST-tagged proteins bound to the beads were eluted 5 to 6 times with buffer containing 50mM Tris HCl and 20mM reduced glutathione, pH8.0. Individual eluted fractions were subjected to SDS-PAGE followed by Coomassie Blue staining and/or immunoblotting, to monitor protein purity and yield.

For His-tagging, cDNA encoding the full length TbRanBPL (GeneID: Tb927.10.8650) or the C-terminal Ran-binding domain only (594nt -1014nt) were sub-cloned into to the pET-28b (+) vector (Novagen). Protein expression, induction and purification were similar to those described in sections 2.8. However, purification of His-tagged proteins was performed with NTA-Ni beads

(QIAGEN, Germany) and protein bound to the beads was eluted with PBS containing 250mM imidazole.

2.9 Bradford assays

Protein concentration was determined using Bradford method in this study. The Bradford method is based on the phenomenon that under acidic conditions, the absorbance maximum for Coomassie Brilliant Blue G-250 shifts from 465nm to 595nm when protein binding occurs. Briefly, 1μl sample or protein standard of known concentration was mixed with 1ml Bradford reagent (0.01% Coomassie Brilliant Blue G250, 5% ethanol and 8.5% phosphoric acid). The absorbance of the mixture was determined by spectrophotometer using 1ml Bradford reagent (BioRad) only as blank. The concentration of sample was determined by the standard curve obtained by plotting OD595nm versus protein standard concentrations.

2.10 Ran activation assay

Ran activation activities were evaluated using a commercially available Ran activation assay kit (Cell Biolabs, USA). This assay takes advantage of the specific binding of human RanBP1 to GTP-Ran, but not GDP-Ran. By monitoring the amount of GTP-Ran bound to RanBP1-coated beads, the Ran activation activity in the cell lysate is quantitatively assessed.

2.10.1 Preparation of parasite lysates

For each assay, 1 x 10^7 of *T. brucei* cells were washed twice with ice-cold PBS and resuspended in 0.5-1ml ice-cold lysis buffer (125 mM HEPES, pH 7.5, 750mM NaCl, 5% NP-40, 50 mM $MgCl_2$, 5 mM EDTA, 10% Glycerol). Cells were lysed by repetitive pipetting and cell lysates were then centrifuged at 14,000 g for 10 min at 4°C to remove cell debris. Volume of each sample was adjusted to 1ml with lysis buffer. For nucleotide loading, 20µl 0.5M EDTA was added to each sample before 10µl GTPγS (100x stock) or 10 µl GDP (100x stock) was added. The tubes were then incubated for 30min at 30°C with agitation. Nucleotide loading was stopped by adding 65µl 1 M $MgCl_2$ to each tube.

2.10.2 Ran pull-down assay

The RanBP1 agarose beads slurry were thoroughly resuspended by vortexing. 40µl slurry was added to each sample prepared in the above section. The tubes were then incubated at 4°C for 1 hour with gentle agitation. The beads were pelleted by centrifugation for 10 seconds at 14,000 X.*g*. After aspirating the supernatant, the beads were washed 3 times with 0.5 ml lysis buffer, centrifuging and aspirating each time. The beads were then resuspended in 40 µl reducing SDS-PAGE sample buffer and denatured at 100°C for 5 min.

Table 2.1 List of vectors used in this study.

Vector	Purpose	Vector origin	Antibiotic resistance		Reporter tag	Linearization site for stable transfection
			E. coli	***T. brucei***		
pGBKT7	Bait plasmid	Clontech	Kanamycine	-	-	-
pXS_2	Constitutive over-expression in procyclic *T. brucei*	Bangs et al., 1996	Ampicillin	Blasticidin	YFP or BB_2	MluI
TOPO	Endogenous replacement of *T. brucei* genes via homologous recombination	Modified pCR4Blunt-TOPO vector Morriswood et al., 2009	Ampicillin	Blasticidin	YFP or BB_2	NsiI or PacI
pLew100	Inducible overexpression in *T. brucei*		Ampicillin	Blasticidin	YFP or BB2	NotI
pZJM	RNAi in *T. brucei*	Wang et al., 2000	Ampicillin	Phleomycin	-	NotI
p2T7	RNAi in *T. brucei*	Wickstand et al., 2002	Ampicillin	Phleomycin/ Blastidin	-	NotI
pET28-a+	Inducible protein expression in *E. coli*	Novagen	Kanamycin	-	Hisx6-	-
pGEX-6P-1	Inducible protein expression in *E. coli*	GE Healthcare	Ampicillin	-	GST	-

Table 2.2 List of antibodies used in this study.

Antibody	Antigen	Origin/Clonality	Reference/Company	Labeled structure in *T.brucei*	Dilution for IB	Dilution for IF
YL1/2	Tyrosinated alpha tubulin	Rat (pAb)	(Kilmartin et al., 1982)	Basal bodies	-	1:1000
Anti-TbLRRP1	TbLRRP1	Mouse (mAb)	Zhou et al., 2010	bilobe	1:2000	1:1000
Anti-Ran	Ran	Mouse (mAb)	Cell Biolabs	Nucleus	1:1000	1:100
KMX-1	β-tubulin	Mouse (mAb)	Roche	Cytoskeleton/Spindle	1:5000	-
Ani-TbVP1L3	TbVP1	Rabbit (pAb)	Lemercier G. et al., 2002	Acidocalcisomes	-	1:500
Anti-TbSKL	TbSKL		Keller et al., 1991			
Anti-TbCentrin4	TbCentrin4	Mouse (mAb)	Shi et al., 2008	Basal bodies and bilobe	-	1:400
Anti-GRASP	TbGRASP65	Rabbit (pAb)	He et al., 2004	Golgi	-	1:1000
Anti-YFP	YFP	Rabbit (pAb)	Abnova	-	1:1000	1:500
Anti-GST	GST	Rabbit (pAb)	GE Healthcare	-	1:2000	-
Anti-HisX6	HisX6	Mouse (mAb)	GE Healthcare	-	1:1000	-

Table 2.3. List of new constructs prepared and primers used in this study

Construct	Insert	Primers	Restriction sites
pGBKT7-LRR	Leucine-rich repeat domain (1-360aa) of TbLRRP1	Forward: GTACTTGAATTCATGCATTCGAAAGCATCCTCT Reverse: CGCATCGGATCCTCAGTATGCGTCGTC	Forward: EcoRI Reverse: BamHI
pGBKT7-CC	Coiled-coil region (480-530aa) of TbLRRP1	Forward: GTA CTTGAATTCGATGCTTCCCCAATGTCC Reverse: CGCATCGGATCCTCACCGACCCTGCATCTCC	Forward: EcoRI Reverse: BamHI
pXS2-YFP-Tb927.10.8650	Full length Tb927.10.8650	Forward: CGGGATCCCGTCGGACCGCCTTAGAGGTGA Reverse: CGGAATTCCGTCACTTAGACTGCTCCTGTGC	Forward: BamHI Reverse: EcoRI
pXS2-Tb927.7.5640-YFP	Full length Tb927.7.5640	Forward: CCCAAGCTTGGATGAGCGAAGACCCAAAC Reverse: CGGCTAGCCGCTCGATGAAAGGCGTATC	Forward: HindIII Reverse: NheI
pXS2-Tb. 927.10.5630-YFP	Full length Tb. 927.10.5630	Forward: CCAAGCTTGGATGGATGATGGTGTAGAAGC Reverse: CTAGCTAGCTAGTTCATGTCGACGTGACAAG	Forward: HindIII Reverse: NheI
pXS2- Tb927.11.10750-YFP	Full length Tb927.11.10750	Forward: CCCAAGCTTGGGATGTCACGCTACATCCCAC Reverse: GGGCTAGCCGCGCGTACTCCAGTGCGCCAT	Forward: HindIII Reverse: NheI
pXS2-Tb927.3.3400-YFP	Full length Tb927.3.3400	Forward: CCAAGCTTGGATGCATGACTCTGTGGGAAC Reverse: TAGCTAGCTAGAACACATTCAGATAGGATAA	Forward: HindIII Reverse: NheI
pXS2-Tb927.6.4140-YFP	Full length Tb927.6.4140	Forward: CCAAGCTTGGATGCCAAACCTCGTTGTCAC Reverse: CGGCTAGCCGAGAGCGAGTGAAATAA	Forward: HindIII Reverse: NheI
pXS2-Tb927.5.150-YFP	Full length Tb927.5.150	Forward: CCCAAGCTTGGGATGCTTAAAATTGCAGCAGT Reverse: CTAGCTAGCTAGGGAGAACACAACACTTAATC	Forward: HindIII Reverse: NheI
pXS2-YFP-Tb927.10.2100	Full length Tb927.10.2100	Forward: CGGGATCCCGGGAAAGGAAAAGGTGCACAT Reverse: CGGAATTCCGTTATTTCTTCGAAGCCTTCACC	Forward: BamHI Reverse: EcoRI

pXS2-YFP-Tb927.7.1060	Full length Tb927.7.1060	Forward: CGGGATCCCGTTTCGCGTTGTGTCGTTTGG Reverse: CGGAATTCCGCTACGATGAGTCTGGGTTGC	Forward: BamHI Reverse: EcoRI
pXS2-Tb927.10.11270-YFP	Full length Tb927.10.11270	Forward: CCAAGCTTGGATGGTGGATCCTTCTGTGCTG Reverse: CTAGCTAGCTAGGTTGTGGACTTGCACCCCCA	Forward: HindIII Reverse: NheI
pXS2-Tb927.9.2110-YFP	Full length Tb927.9.2110	Forward: CCCAAGCTTGGGATGTCACGCAATACAAAGGA Reverse: CTAGCTAGCTAG GTTCGCTTCGGGATTCTTAC	Forward: HindIII Reverse: NheI
TOPO-YFP- Tb927.10.8650	500 bp 5' UTR and 500 bp 5' end of coding sequence	UTR Forward: CCTTAATTAAGGTCTGGAGCTGGAGCTTGA Reverse: CCAAGCTTGGTCGCTAACAGGTGTCGCTCT 500 bp 5' coding sequence Forward: CGGGATCCCGTCGGACCGCCTTAGAGGTGA Reverse: TGCATGCATGCACTTAGACTGCTCCTGAGTT	UTR Forward: PacI Reverse: HindIII 500 bp 5' coding Forward: BamHI Reverse: NsiI
pLew100-YFP- Tb927.10.8650	Full length Tb927.10.8650	Forward: GAAGATCTTCTCGGACCGCCTTAGAGGTGA Reverse: CGGGATCCC TCACTTAGACTGCTCCTGTG	Forward: BgIII Reverse:BamHI
P2T7-Tb927.10.8650 and pZJM-Tb927.10.8650	RNAi fragment as identified by the RNAit program (Redmond et al., 2003)	Forward: TGCTCTAGAGCACGCAATGACTGCAACTGACT Reverse: TGCTCTAGAGCACATTCGCTCCCGTGTATTTT	Forward: XbaI Reverse: XbaI
P2T7-TbRan and pZJM- TbRan		Forward: TGCTCTAGAGCAATGTCCATCCGCTCACTTTC Reverse: TGCTCTAGAGCATGAAGTGCCTGCAACTGTTC	Forward: XbaI Reverse: XbaI
P2T7-TbLRRP1		Forward: CTAGTCTAGACGATGTGAAATG Reverse: CTAGTCTAGATACGGTTTGGGGTA	Forward: XbaI Reverse: XbaI

CHAPTER 3: Results

3.1 Domain analyses of TbLRRP1

TbLRRP1 was identified as a bilobe component in a comparative proteomics screening for flagellum associated proteins (Zhou et al., 2010). The 713-amino acid protein comprises of a leucine-rich repeats-containing domain followed with a coiled-coil region near the C-terminus (Fig 1.4). The leucine-rich repeats (LRR) in TbLRRP1 belong to ribonuclease inhibitor subtype (Kobe et al., 2001), which form similar structure motif to the LRR present in the GTPase activating protein (RanGAP) rna1P (Hillig RC et al., 1999). Rna1P interacts directly with small GTPase Ran through its LRR and facilitates Ran activation, a critical regulatory process for nucleocytoplasmic transport (Seewald et al., 2002).

To understand the domain function in bilobe targeting, different truncated versions of TbLRRP1 were fused to YFP reporter and expressed in procyclic *T.brucei* (Fig.3.1). The LRR domain did not bear any localization information and YFP- LRR was found distributed throughout the cytoplasm. The coiled-coil domain alone however, was necessary and sufficient in mediating bilobe localization, possibly through its protein oligomerization activity (Burkhard et al., 2001).

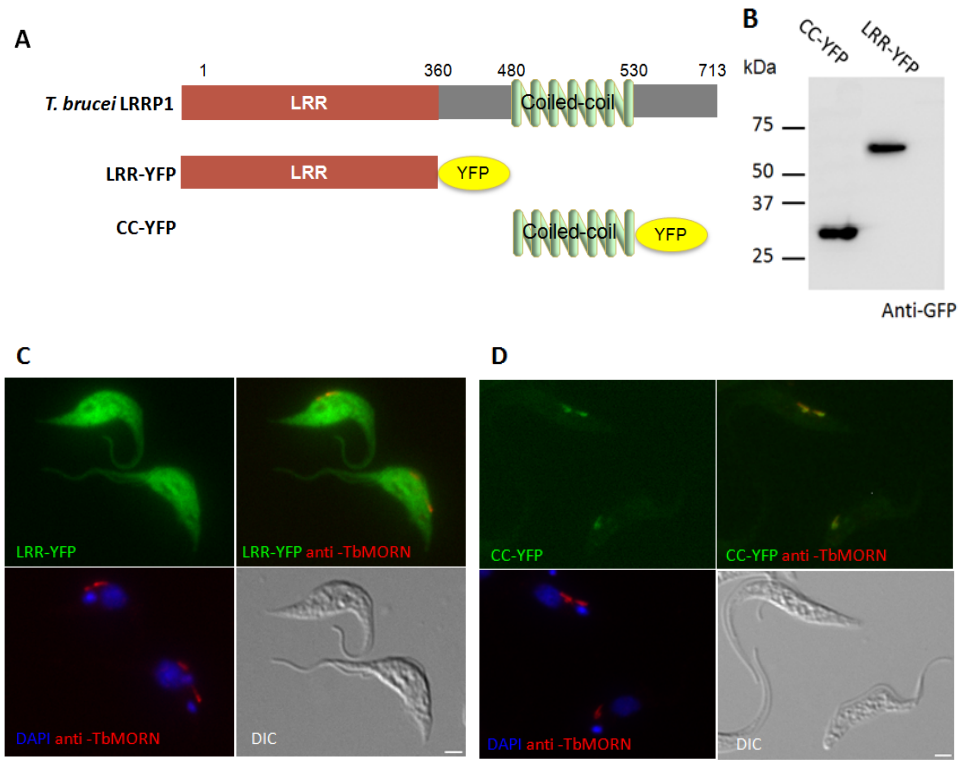

FIGURE 3.1. The 50aa coiled-coil motif of TbLRRP1 is sufficient and necessary for bilobe targeting. (A) The schematic represents the truncation mutants of TbLRRP1. (B-D) TbLRRP1 truncation mutants were expressed in procyclic *T. brucei* and the expression was examined by immunoblots using anti-GFP and immunofluorescence microcopy. Whereas LRR-YFP was distributed throughout the cell, cc-YFP that contained only the 50aa coiled-coil region of TbLRRP1 localized specifically to the bilobe, colocalizing with the anti-TbMORN1 antibody. Scale bar=2µm.

3.2 Yeast-two-hybrid screening for TbLRRP1-interacting proteins

To further investigate the molecular function and mechanism of TbLRRP1, a yeast-two-hybrid screening was performed to search for *T. brucei* proteins that interact with TbLRRP1. In doing this, a procyclic *T. brucei* cDNA library with total of ~ 6.5× 10^5 colonies with a 60-fold coverage of the *T.brucei* coding

genome (9068 genes with an average length of ~1500bp/gene) was constructed (Zhang, 2012). Screening was performed using either the LRR or the coiled-coil domain as bait.

3.2.1 Auto activation test for LRR- and coiled-coil-containing bait constructs

Bait proteins with high auto activity, i. e. high intrinsic activity to initiate transcription of reporter genes, cannot be used for yeast-two-hybrid screening. Therefore, both LRR- and coiled-coil-containing bait proteins were tested for any possible auto activity. Two reporters for yeast two-hybrid screening, HIS3 and ADE2, are necessary for biosynthesis of essential nutrients; histidine (His) and adenine (Ade). Yeast strain YH187 expressing bait-plasmids alone did not grow on medium lacking either His or Ade (data not shown), indicating that neither BD-LRR nor BD-coiled-coil could initiate transcription of ADE2 or HIS3 alone, validating these bait constructs for further screening.

3.2.2 Summary of yeast-two-hybrid screening results

Yeast mating was performed between yeast strain Y187 that harbored either the LRR or the coiled-coil domain in bait plasmid, and yeast strain AH109 that was transformed with *T. brucei* cDNA library as prey. Mating between Y187 cells harboring bait construct and AH109 cells transformed with empty vector was

used as negative control. As expected, no colonies appeared in the control experiment while diploids representing interactions between bait and prey proteins were selected with high-interagency medium (SD/-His/-Ade/-Trp/-Leu). To eliminate false positive Ade^+/His^+ colonies, all colonies obtained on high-interagency medium were streaked out on fresh SD/-His/-Ade/-Trp/-Leu/X-α-Gal master plates in a grid fashion and incubated for 4-5 more days. A total of 70 positive blue colonies resulted from three independent yeast mating experiments for LRR (Fig 3.2). To identify the genes (and thus proteins) responsible for the positive two-hybrid interaction, the cDNA inserts were rescued by colony PCR and sequenced using either T7 primer and/or matchmaker AD LD- insert screening amplimer set (Clontech). A total of 53 PCR fragments were successfully sequenced. Among these, 7 fragments encoded ribosomal proteins, which are frequently observed in yeast two-hybrid screenings and generally treated as false positives (Hengen, 1997). The remaining 46 PCR fragments represented 27 different proteins listed in Table 3.1, which were classified according to their cellular distribution and functional annotation. Proteins highlighted in yellow were further analyzed for cellular localization.

Interestingly, for the coiled-coil domain, most inserts recovered (12 out of 17 PCR fragments sequenced) encoded a 20S ribosomal protein. Only 5 non-ribosomal, non- redundant genes were identified from two separate mating experiments. All 5 genes are listed in Table 3.2.

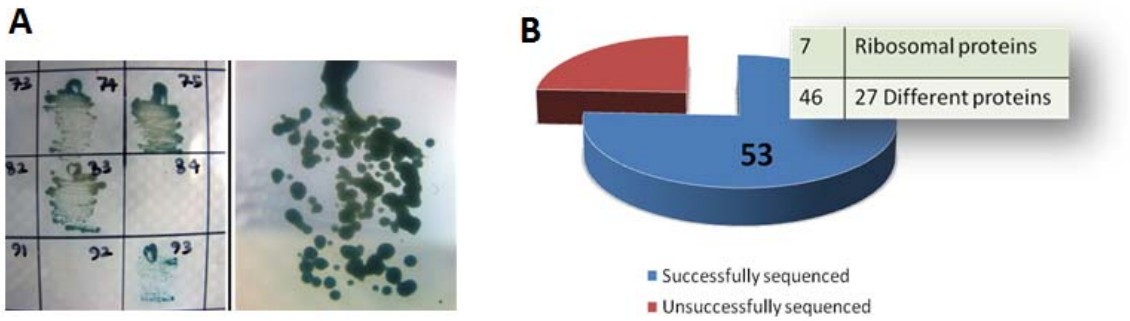

FIGURE 3.2 Yeast-two-hybrid screening to identify binding partners of TbLRRP1 (A) Positive Ade^+/His^+ colonies were streaked out on SD/-His/-Ade/-Trp/-Leu/X-α-Gal master plates in a grid fashion (left) and positive blue colonies appeared after 6 days (right). **(B)** More than 70 colonies were recovered and prey-coding cDNAs were amplified using matchmaker LD/AD amplimer set. cDNA from 53 colonies were successfully sequenced (blue).

Table 3.1. List of non-redundant genes identified by yeast two-hybrid screening for LRR-interacting proteins.

Classification	Gene ID	Annotation	Hit number
Hypothetical proteins of unknown cellular localization and function	Tb927.11.5660	Hypothetical protein	1
	Tb927.10.5630		1
	Tb927.11.10840		1
	Tb927.7.1060		1
	Tb927.9.2110		3
	Tb927.11.16070		1
	Tb927.5.150		1
	Tb09.211.2350		1
Hypothetical proteins containing known functional domains	Tb927.3.1970	Hypothetical protein, cointaining DFP; DNA / pantothenate metabolism flavoprotein	2
	Tb927.10.8650	Hypothetical protein, containing RanBP1 domain	1
	Tb927.7.5640	Hypothetical protein, Containing D111/G patch domain	1
	Tb927.11.3160	Tro-A like superfamily	1

Nuclear proteins	Tb927.11.10750	Putative pre-mRNA-splicing factor CWC22	1
	Tb927.5.3970	Putative adenylate kinase	3
	Tb927.1.350	Putative retrotrasposon hot spot protein	3
	Tb927.7.1370	Putative spliced leader RNA PSE-promoter transcription factor	2
	Tb927.1.540	Putative DNA-directed RNA polymerase III, RPC128	2
Cytoplasmic proteins	Tb927.10.2100	elongation factor 1-alpha,EF-1-alpha (TEF1)	4
	Tb927.10.11270	Putative RNA binding protein (RBP23)	1
	Tb927.11.5140	Putative, Ubiquitin carboxyl-terminal hydroxylase	1
	Tb927.3.3400	Putative Kinesin	1
Paraflafellar rod proteins	Tb927.6.4140	Putative paraflagellar rod component,PFC4	1
Glycosomal proteins	Tb927.8.3530	glycerol-3-phosphate dehydrogenase [NAD^+]	2
	Tb927.10.2020	Putative hexokinase 2	3
Mitochondrial proteins	Tb927.10.4310	Putative prohibitin2 (PHB2)	1
	Tb927.8.3330	Mitochondrial carrier protein	1

Genes highlighted in yellow were further analyzed for cellular localization.

Table 3.2. List of non-redundant genes identified by yeast two-hybrid screening for Coiled-coil-interacting proteins.

Classification	Gene ID	Annotation	Hit number
Hypothetical protein	Tb927.6.3930	TPR-like protein	2
Mitochondrial protein	Tb09.160.2970	mitochondrial RNA editing ligase, KREL1	1
	Tb927.6.217	Putative co-chaperone GrpE	1
Cytoplasmic protein	Tb10.70.5830	Actin-Like protein putative	1
Nuclear proteins	Tb927.1.350	Putative, retrotransposon hot spot (RHS) protein	2

Gene highlighted in yellow was further analyzed for cellular localization.

3.2.3 Sub-cellular localization of selected, putative binding partners of TbLRRP1

Among the putative TbLRRP1 binding proteins (Tables 3.1 and 3.2), about 30% of the candidates represented previously uncharacterized proteins with unknown functions, making the selection for protein candidates for further characterization challenging. A detailed domain analysis for each protein candidate was performed using bioinformatics methods. This allowed rapid screening of protein candidates with interesting domain organization or domain function, which may be related to TbLRRP1 function and localization. The sub-cellular localization of these proteins (highlighted in yellow, Tables 3.1 and 3.2) were then examined using a YFP-tagging approach in procyclic *T.brucei*.

Full length DNA coding sequences were amplified by PCR, fused with YFP and over-expressed in procyclic *T.brucei*. The intracellular localization of these proteins is summarized in Table 3.3. Disappointingly, not a single protein candidate exhibited clear localization to the bilobe, where TbLRRP1 resides.

TABLE 3.3 Sub cellular localization of selected protein candidates identified by yeast-two-hybrid screening.

Protein name	Accession number	Gene length (bp)	YFP-tagged N or C-terminally	Transiently or stably expressed	Sub-cellular localization
Hypothetical protein	Tb927.10.8650	1014	N	Stable	Cytoplasmic
Hypothetical protein	Tb927.10.5630	558	C	Stable	Cytoplasmic
Hypothetical protein	Tb927.7.5640	816	C	Stable	Basal bodies
Hypothetical protein	Tb927.9.2110	342	C	Transient	Cytoplasmic
Hypothetical protein	Tb 927.7.1060	1465	N	Transient	Cytoplasmic
Hypothetical protein	Tb927.5.150	816	C	Stable	Glycosomes
Putative kinesin	Tb927.3.3400	1737	C	Transient	Cytoplasmic
Elongation factor 1-alpha,EF-1-alpha (TEF1)	Tb927.10.2100	1350	N	Transient	Cytoplasmic
Putative paraflagellar rod component,PFC4	Tb927.6.4140	348	C	Stable	Cytoplasmic
Pre-mRNA-splicing factor, CWC22	Tb11.01.2520	1746	C	Transient	Nucleolus
putative RNA-binding protein, (RBP23)	Tb927.10.11270	729	C	Transient	Cytoplasmic

3.3 Characterization of a hypothetical protein containing Ran-binding domain

Although the YFP-localization study did not reveal useful information in narrowing down the list, one putative LRR-binding candidate, encoded by Tb927.10.8650, was of particular interest among other candidates. This 337-amino acid hypothetical protein contains a putative Ran-binding domain (with an E value of $1.66x10^{-10}$) in the C-terminal region, suggesting that it may bind to Ran. YFP-tagged Tb927.10.8650 exhibited a cytoplasmic distribution in cells

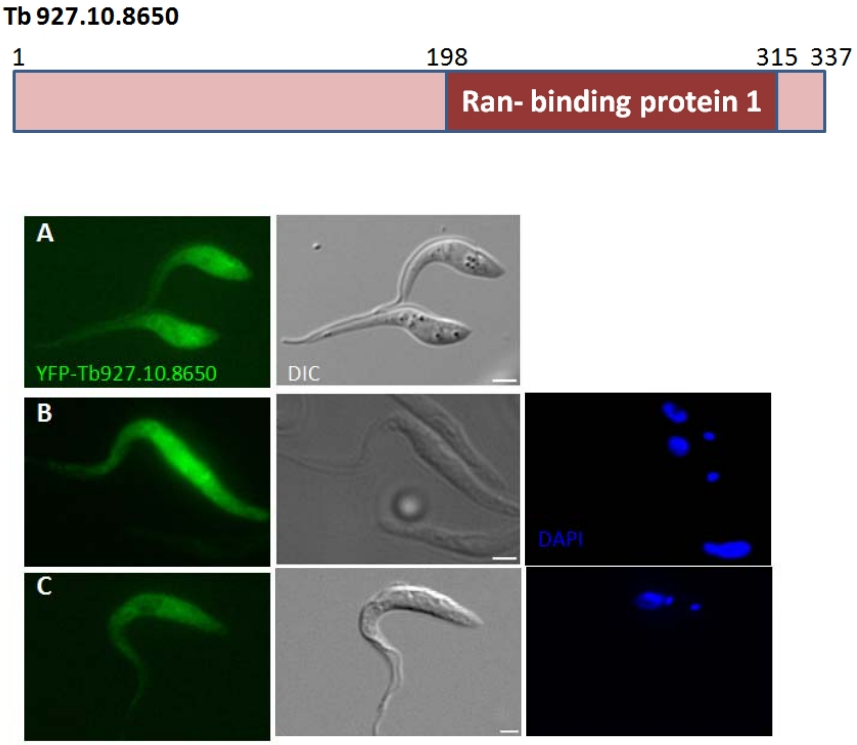

FIGURE 3.3 Sub-cellular localization of hypothetical protein encoded by Tb927.10.8650. pXS2-YFP and pLew-100-YFP vectors were used to over-express the protein as YFP-tagged fusions. (A) Live YTat1.1 cells transiently transfected with pXS2-YFP-Tb927.10.8650 showed YFP signal throughout the cytoplasm. (B) Cells in (A) were fixed in PFA and YFP signal was observed in the cytoplasm. (C) Similar cytoplasmic distribution was also observed in cells containing pLew100-YFP-Tb927.10.8650 for inducible expression of pXS2-YFP-Tb927.10.8650. Scale bar=2µm.

expressing the fusion, transiently expressing the fusion, transiently or inducibly (Fig 3.3). No specific enrichment of this protein was observed at the bilobe.

3.3.1 An introduction to Ran GTPase

Ran is an abundant Ras-like small GTPase. It is initially characterized for its role in modulating nucleocytoplasmic transport of macromolecules across the nuclear envelope (Moore et al., 1994). Later studies also find Ran GTPase involved in mitotic spindle and nuclear envelope re-assembly during the cell cycle (Gruss et al., 2004; Ciciarello et al., 2007). More recently, Ran GTPase activity is also linked to regulated ciliary protein entry (Dishinger et al., 2010). Like all Ras-like GTPase family members, Ran GTPase functions as a molecular switch cycling between the GTP-bound form and the GDP-bound form (Fig 3.4). Ran's association with different cellular proteins depends upon the nucleotide that it is bound to. Furthermore, GTP-bound Ran is specifically enriched in the nucleus while GDP-bound Ran is enriched in the cytoplasm (Joseph, 2006). This steep and asymmetrical distribution is critically required for the directionality of nucleocytoplasmic trafficking, and is thus tightly regulated by two GTPase regulatory proteins namely Guanine Exchange Factor (GEF) and GTPase Activating Protein (GAP). RanGEF is able to trigger the exchange of GDP to GTP in Ran GTPase, whereas RanGAP is cable of catalyzing the hydrolysis of GTP to GDP (Bos et al., 2007) (Fig 3.4).

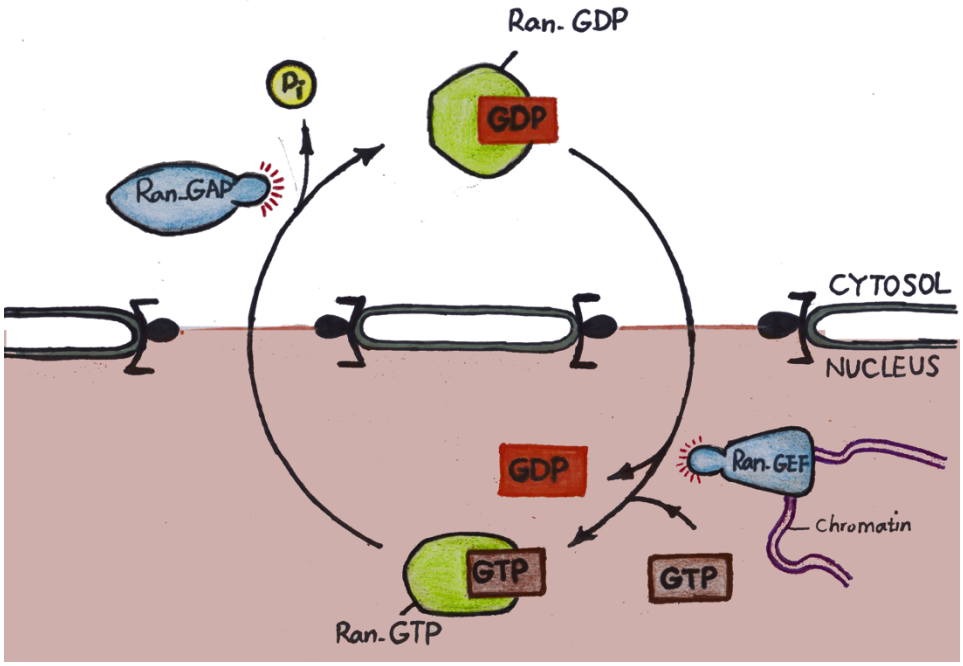

FIGURE 3.4 The Ran GTPase cycle. The Ran gradient in the cell is achieved by an asymmetric distribution of the Ran regulators. RCC1, the Ran guanine-nucleotide exchange factor (Ran-GEF) is bound to chromatin in the nucleus and promotes the dissociation of GDP from Ran and allows the binding of GTP. Ran in the nucleus is therefore predominantly in the GTP-bound form. Once RanGTP leaves the nucleus (together with its cargo), the RanGTPase-activating protein (RanGAP) induces GTP hydrolysis by Ran in cooperation with two Ran-binding proteins (RanBP1 and RanBP2), thus returning the Ran to GDP-bound form, which is competent for nuclear import. (The artwork attained by pencil drawing.)

3.3.2 Characterization of a Ran GTPase homolog in *T.brucei*

Ran has been identified bioinformatically in many protozoan parasites including Giardia, apicomplexans and trypanosomatids (Chen et al., 1994; Frankel and Knoll, 2008; Casanova et al., 2008). In *T. brucei*, a single homolog of Ran GTPase (rtb2) is encoded by Tb927.3.1120 (Field et al., 1995). Stable expression of a YFP fusion to *T. brucei* Ran (YFP-Ran) resulted in Ran localization to both

the nucleus and the cytoplasm, with predominantly nuclear staining present throughout the cell cycle (Fig 3.5). While this localization is similar to that observed in yeast and mammalian cells, it is different to the peri-nuclear localization observed for *L. major* Ran (Casanova et al., 2008) and the even distribution of *T. gondii* Ran throughout the cell (Frankel et al., 2008).

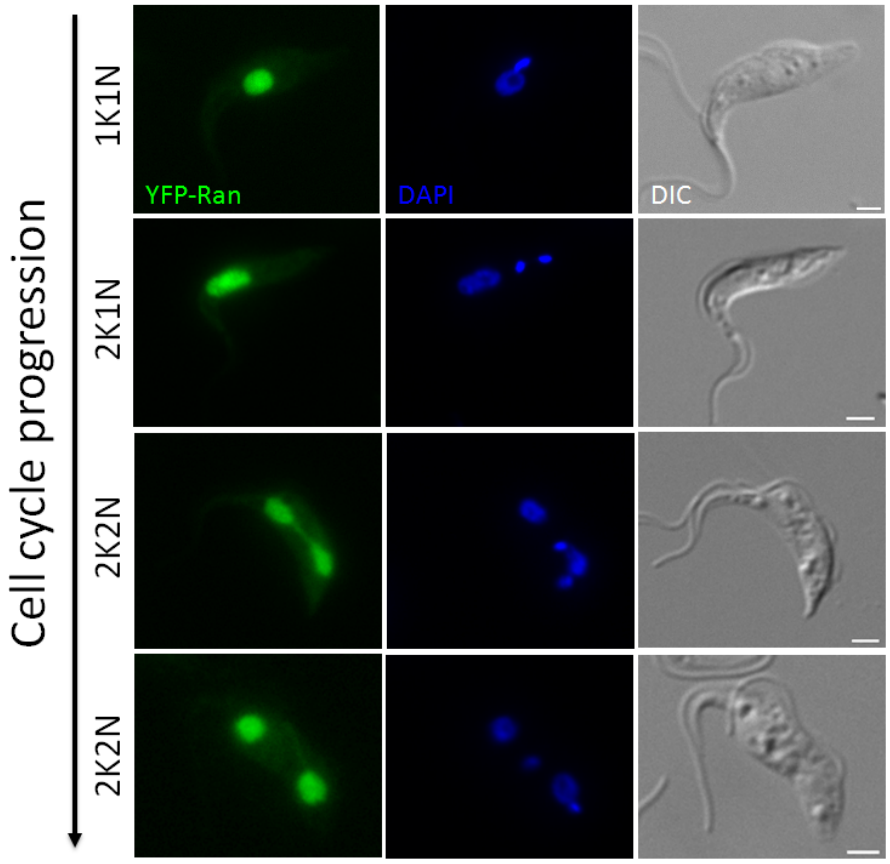

FIGURE 3.5 Cellular localization of *T. brucei* RanGTPase during the cell cycle. 29.13 cells stably over-expressing the YFP-Ran exhibited predominant YFP localization in the nucleus in addition to cytoplasmic signal. As the cells progressed through the 'closed' mitosis, Ran nuclear distribution remained intact. Scale bar= 2µm.

The subcellular localization of Ran in *T. brucei* was further verified using a monoclonal antibody (mAb) raised against human Ran (Cell Biolab, USA). This anti-Ran mAb cross reacted to *T. brucei* Ran and labeled it specifically on immunoblots (Fig 3.6).

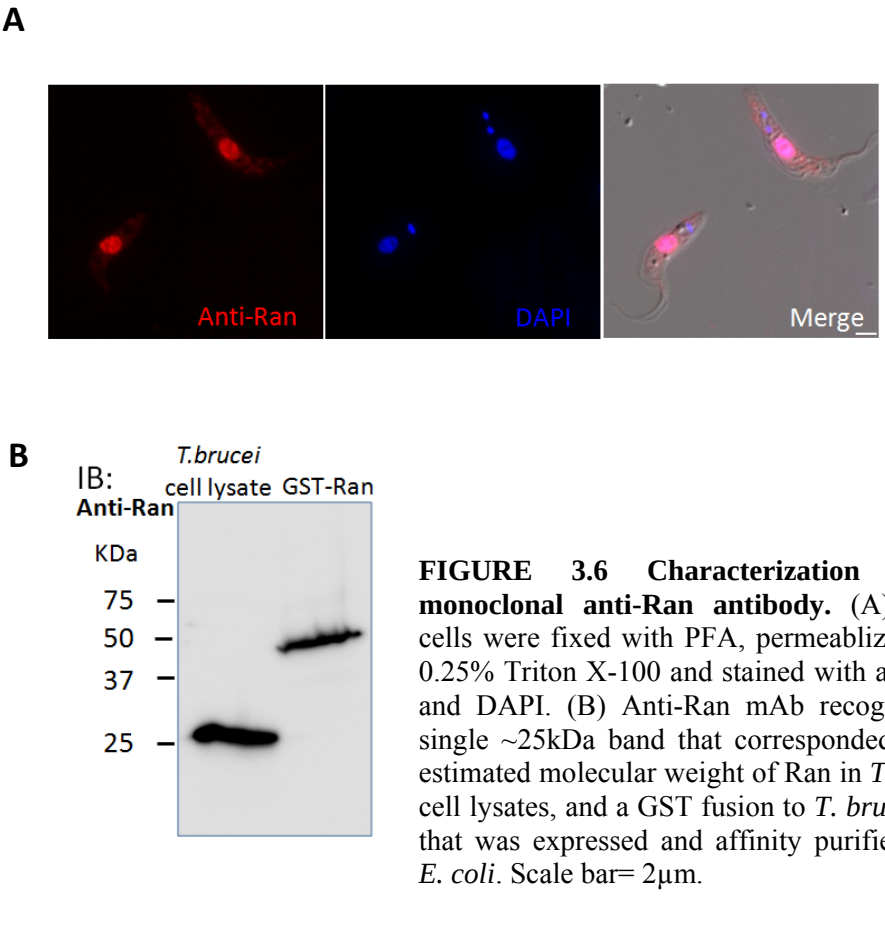

FIGURE 3.6 Characterization of a monoclonal anti-Ran antibody. (A) 29.13 cells were fixed with PFA, permeablized with 0.25% Triton X-100 and stained with anti-Ran and DAPI. (B) Anti-Ran mAb recognized a single ~25kDa band that corresponded to the estimated molecular weight of Ran in *T. brucei* cell lysates, and a GST fusion to *T. brucei* Ran that was expressed and affinity purified from *E. coli*. Scale bar= 2µm.

3.3.3 Characterization of two *T.brucei* Ran mutants

Next I examined two mutant forms of *T. brucei* Ran, Ran G21V in which Gly^{21} was replaced with Val and Ran T26N. By analogy to the Ras mutants, Ran G21V mimics a permanently active GTP-locked mutant and Ran T26N a permanently inactive GDP-locked state. Correspondingly, YFP-Ran T26N localized primarily

in the nucleus, and YFP-Ran G21V showed reduced labeling in the nucleus and more prominent distribution in the cytosol (Fig. 3.7). These results confirmed that *T. brucei* Ran behaved like an authentic Ran.

It has been shown by others in the lab (He's group, unpublished results) that Ran is essential for *T. brucei* viability. Cells lacking Ran exhibited mitotic arrest, where nuclear division was inhibited, leading to a significant accumulation of 2K1N cells. This is however, distinct to the effect observed in *T. brucei* transiently overexpressing the above Ran mutants. As shown in Fig 3.8, the percentage of 1K2N cells increased in cells expressing either Ran T26N or Ran G21V, suggesting an inhibition of kinetoplast segregation in these cells. Consistently, stable expression clones could not be obtained for either mutant. It is, however, not clear why expression of the Ran mutants resulted in phenotypes different to Ran depletion.

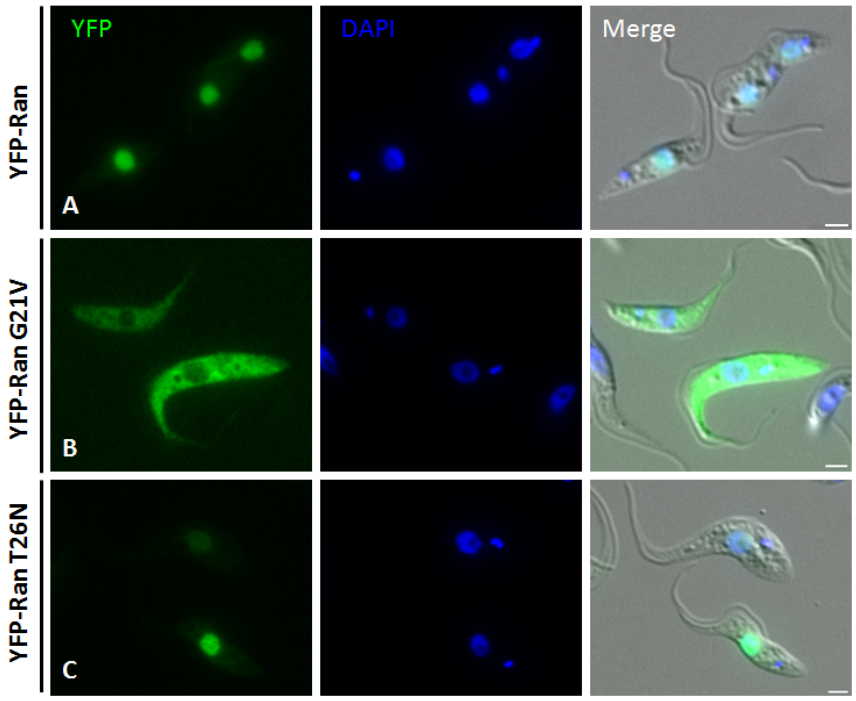

FIGURE 3.7 Cellular localization of TbRanGTPase mutants. 29.13 cells transiently expressing YFP fusion to wild type Ran (A), GTP-locked Ran G21V (B), and GDP-locked Ran T26N (C) Wild-type TbRan localized to the nucleus and weakly to the cytoplasm. GTP-locked form of TbRan localized to the cytoplasm excluded from the nucleus, while GDP-locked form mutant localized to the nucleus. Scale bar= 2µm.

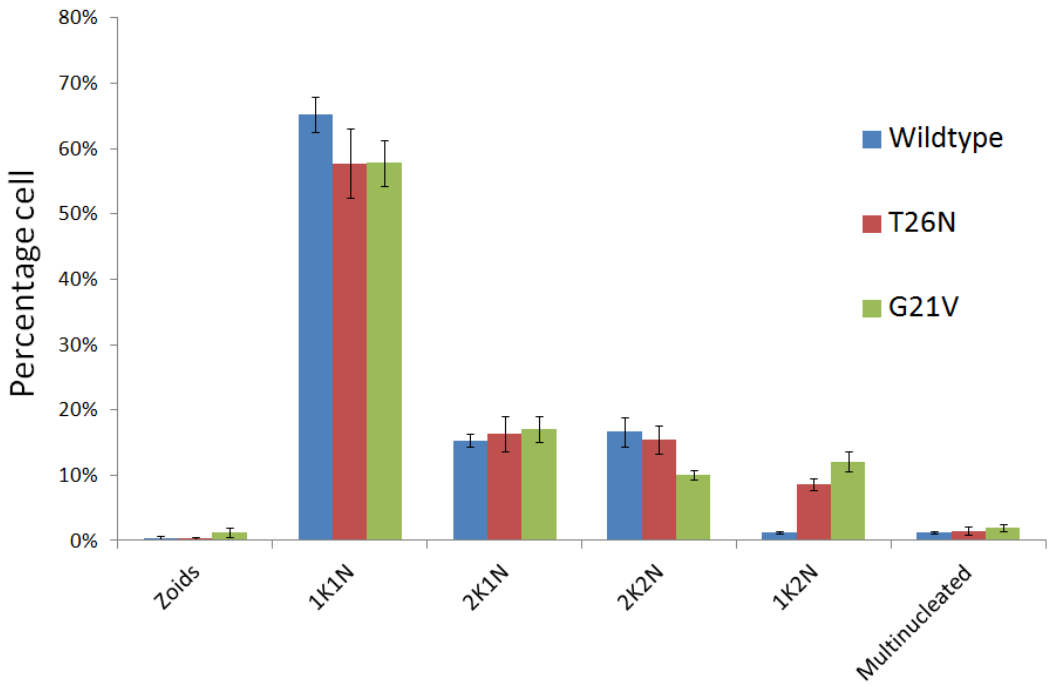

FIGURE 3.8 Effect of TbRan mutations on *T.brucei* cell cycle. Cells transiently expressing YFP-Ran, YFP-Ran T26N and YFP-Ran G21V were monitored for percentage of 1K2N cells in the whole cell population increased in cells expressing either TbRan mutated forms, G21V and T26N, inhibition of kinetoplast segregation.

3.4 Tb927.10.8650 encodes a new Ran-binding protein

To examine the interaction between the hypothetical, Ran binding domain-containing protein encoded by Tb927.10.8650, a pull down analysis was performed using bacterially expressed His-tagged Tb927.10.8650 and GST-tagged Ran. GST-Ran was also preloaded with non-hydrolyzable GTP-γ-S or GDP to lock Ran in the GTP or GDP-bound states. As shown in Fig 3.9, Tb927.10.8650, either the full-length protein or the C-terminal region containing

the Ran-binding domain, both interacted with Ran in a GTP-dependent fashion. The gene product of Tb927.10.8650 was thus renamed *T. brucei* RanBPL for RanBP-like protein. RanBPL showed little homology (~8% identity and 13 % similarity) to the putative RanBP1 (encoded by Tb11.02.0870) previously characterized in *T. brucei* (Casanova et al., 2008).

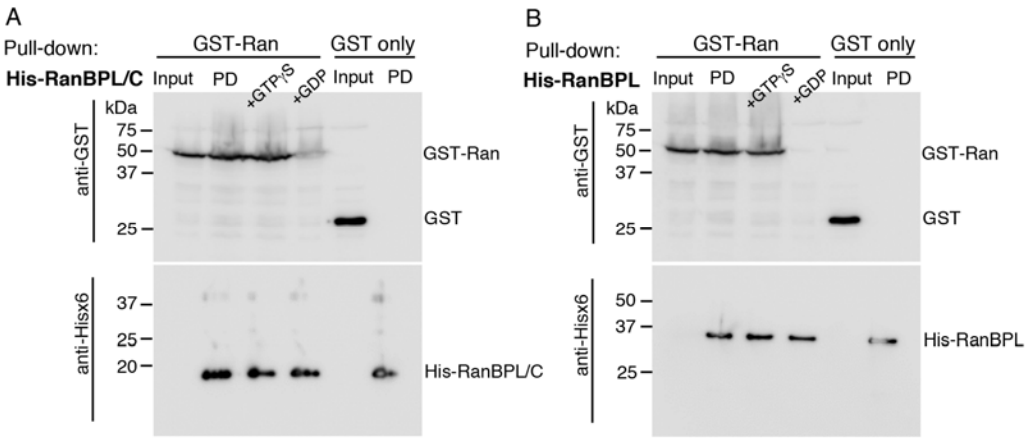

FIGURE 3.9. Tb927.10.8650 interacts with Ran through its Ran-binding domain in a GTP-dependent fashion. His-tagged full-length RanBPL (A) or the C-terminal region containing the Ran-binding domain (RanBPL/C) (B) were immobilized to Ni^{++}-NTA beads and used in pull-down assays, incubating with bacterial cell lysates expressing GST-Ran or GST only. As controls, bacterial lysates expressing GST-Ran were preloaded with GTPγS or GDP. RanBPL, full length or RanBPL/C, both interacted with GST-Ran but not GST only, in a GTP-dependent manner. 2% bacterial lysates were loaded as input and entire pull-down products were loaded in PD lanes.

3.5 Ran, RanBPL and TbLRRP1 form a complex

As RanBPL was initially characterized by yeast-two-hybrid screening as a putative TbLRRP1-interacting protein, the interaction between RanBPL and TbLRRP1 was then tested. Neither the full-length LRRP1 nor the LRR-containing N-terminal domain was soluble when expressed as bacterial fusion protein, interaction between TbRanBPL and TbLRRP1 was therefore examined using a pulled-down analysis, by incubating *T. brucei* cell lysates with His- RanBPL immoblized on beads (Fig 3.10A). As shown in Fig 3.10B, His-RanBPL pulled down both YFP-Ran and endogenous LRRP1, confirming the yeast-two-hybrid screening result as well as the interaction between RanBPL and Ran. Interestingly, both the full-length His-RanBPL, and the C-terminal region containing the Ran binding domain, failed to pull down LRRP1 in Ran-RNAi cells, though expression of LRRP1 in these cells was normal (Fig 3.11). These results suggested that Ran, RanBPL and LRRP1 formed a complex in vivo, and the interaction between RanBPL and LRRP1 relied on the presence of Ran.

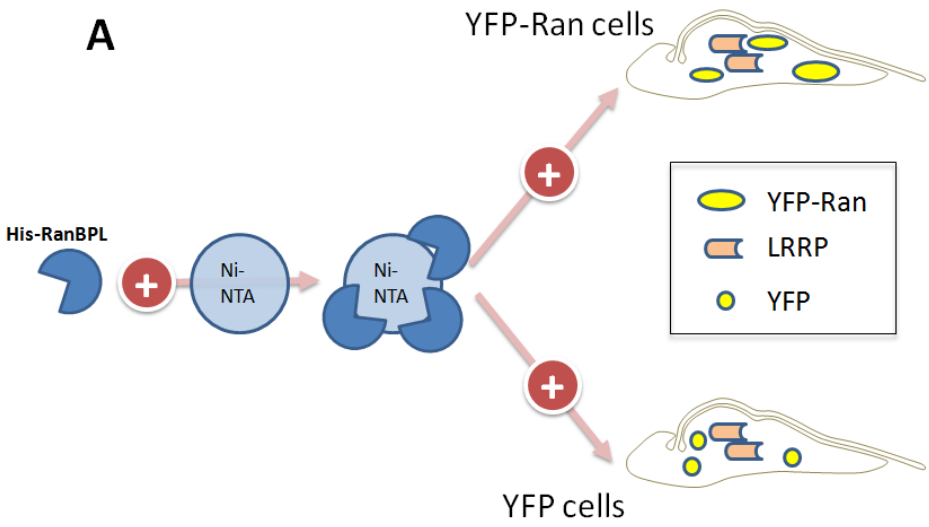

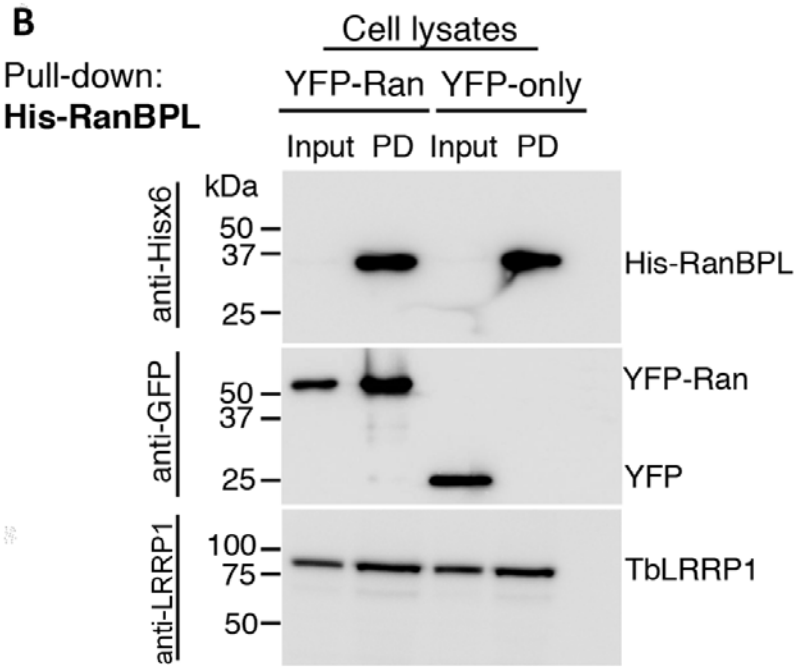

FIGURE 3.10 In-vitro isolation of RanBPL-Ran-TbLRRP1 complex. (A) To confirm the binding of RanBPL to Ran and TbLRRP1, His-TbRanBPL immobilized on beads was incubated with cell lysates containing stably expressed YFP-TbRan or YFP only. (B) His-RanBPL specifically pulled down YFP-Ran but not YFP only. Endogenous TbLRRP1 was pulled down in the same experiments, confirming the presence of RanBPL, Ran and TbLRRP1 in the same protein complex.

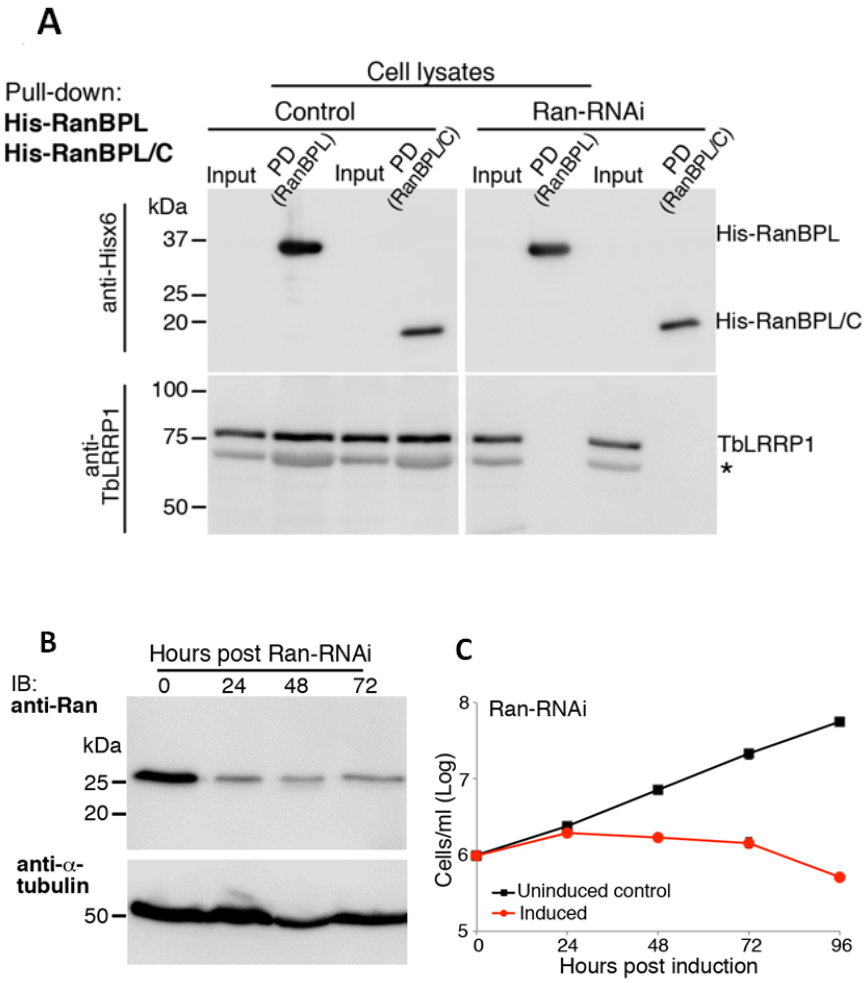

FIGURE 3.11 the interaction between RanBPL and TbLRRP1 relies on the presence of Ran. (A) Both His-RanBPL and His-RanBPL/C failed to pull down TbLRRP1 in Ran-RNAi cell lysates, though expression of TbLRRP1 was unaltered by Ran-depletion (compare the input lanes for control and Ran-RNAi cells). '∗' indicates a non-specific band often observed in anti-TbLRRP1 blots. (B) Depletion of the Ran protein on immunoblots over the course of tetracycline induction. (C) Proliferation of the Ran-depleted cells ceased ~24 hours post-induction.

3.6 TbLRRP1 functions in Ran regulation

3.6.1 TbLRRP1 depletion disrupted the Ran distribution between nucleus and cytoplasm

The interaction between Ran, RanBPL and TbLRRP1 is reminiscent of the Ran-RanBP-RanGAP ternary complex previously characterized in human and yeast cells (Seewald et al., 2002). RanGAP directly interacts with Ran through the LRR domain, which belongs to the same RI-like class as the LRR found in TbLRRP1.

I therefore hypothesized that TbLRRP1, which localizes to the bilobe and is essential for cell viability, functioned as a RanGAP. To test this hypothesis, the effects of TbLRRP1 on Ran activity both in vivo and in vitro were investigated. First, YFP-Ran was stably expressed in a stable TbLRRP1-RNAi cell line previously constructed (Zhou et al., 2010).

Despite several cloning attempts, a clonal population with homogenous YFP-Ran expression could not be obtained. Many cells had no detectable YFP expression (Fig 3.12A). Upon induction of TbLRRP1 depletion with tetracycline, redistribution of YFP-Ran from nucleus to cytoplasm was observed in >50% of the cells as early as 16 hours post TbLRRP1-RNAi (Fig 3.12A and B). Cells with cytoplasmic YFP-Ran continued to increase over the course of induction (Fig 3.12B) Given that the onset of organelle duplication and cell division phenotypes were only observed later at ~48 hours post-induction (Zhou et al., 2010), disruption of intracellular Ran distribution appeared to be a primary effect of LRRP1. Interestingly, in a small fraction of TbLRRP1-depleted cells (~10% at

24h post-induction), YFP-Ran was found in cytoplasmic punctate structures. The nature of these puncta was not clear, but they were reminiscent of the punctate structures that small RNA-binding protein La accumulated when nuclear import was inhibited upon transient depletion of ATP (Marchetti et al., 2000), suggesting a possible effect of TbLRRP1-RNAi on nuclear import.

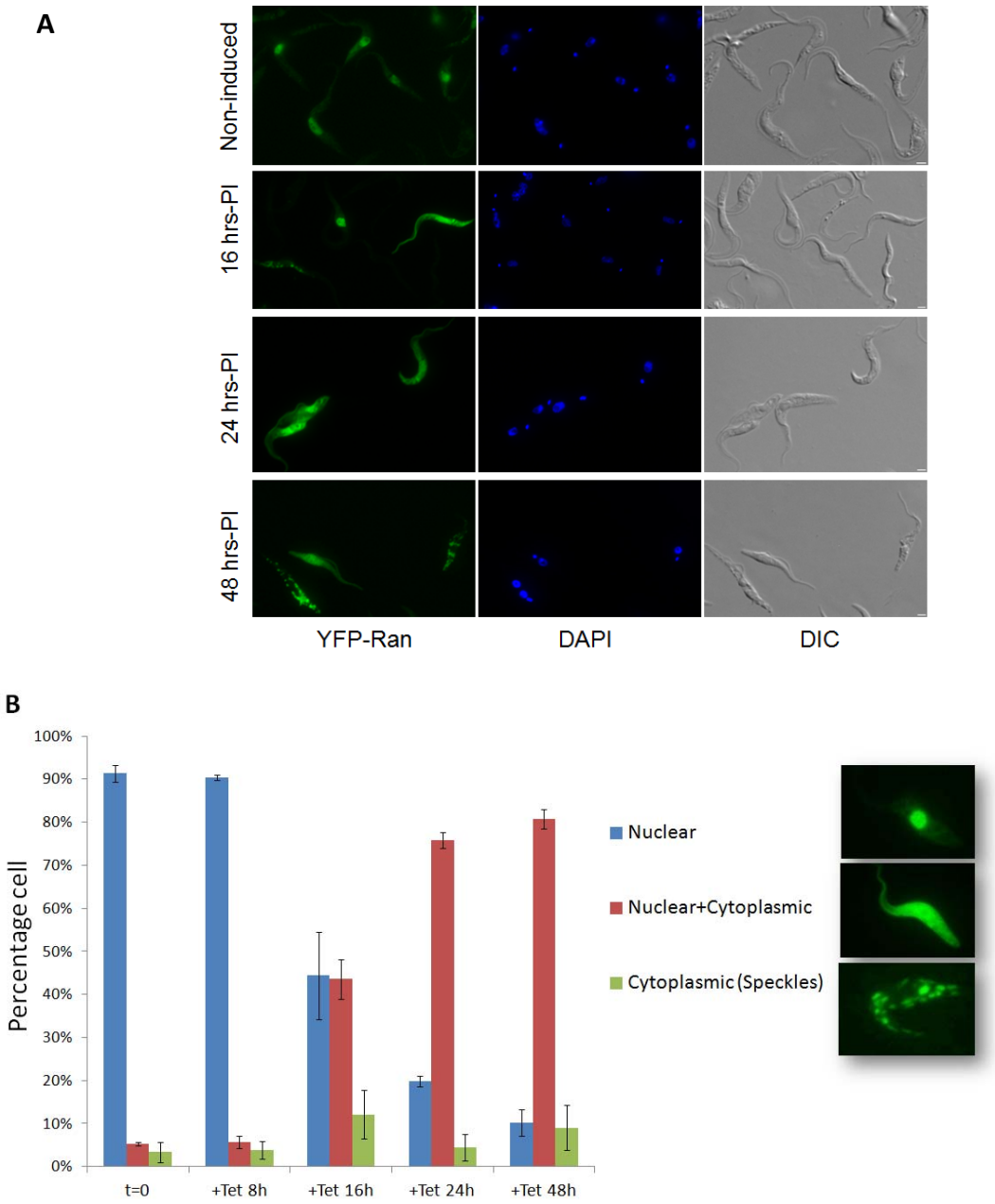

FIGURE 3.12 TbLRRP1 depletion disrupted Ran distribution in the nucleus and the cytoplasm (A) To study the effect of TbLRRP1 depletion on Ran gradient, stable TbLRRP1-RNAi cells were doubly transfected with pXS2-YFP-TbRan. Stable clonal population with ~50% cells showing detectable YFP-TbRan expression was selected, and induced with tetracycline for TbLRRP1-RNAi. Changes in YFP-Ran localization were observed as early as 16 hours post induction, (B) Quantitative analysis of TbLRRP1-depletion on Ran localization. Scale bar=2μm.

3.6.2 TbLRRP1 is required for RanGTP hydrolysis

TbLRRP1 was then analyzed for its function in RanGTP hydrolysis, using a commercially available Ran activation assay (Cell Biolab). In this assay, the selective binding of a human RanBP1 to GTP-bound Ran was used as a read out for RanGTP hydrolysis activity in cell lysates (Fig 3.13A). Agarose beads coated with human His-RanBP1 were incubated with lysates of cells induced for TbLRRP1-RNAi or not. Uninduced cell lysates preloaded with non-hydrolyzable GTP-γ-S or GDP to lock Ran in the GTP or GDP-bound states were also used as controls. As shown in Fig 3.13B, human RanBP1 bound to *T. brucei* Ran in a GTP-dependent fashion. Whereas GTP- γ -S enhanced the binding, GDP completely inhibited it, verifying the binding selectivity of human RanBP1 to *T. brucei* GTP-bound Ran. In cell lysates lacking TbLRRP1, binding of human RanBP1 to Ran was also enhanced as compared to control lysates containing TbLRRP1, indicating reduced Ran activation (therefore more Ran in the GTP-bound state) in the absence of TbLRRP1. Similar results were observed when *T. brucei* RanBPL was used to replace human RanBP1 in the Ran activation assay (Fig 3.13D).

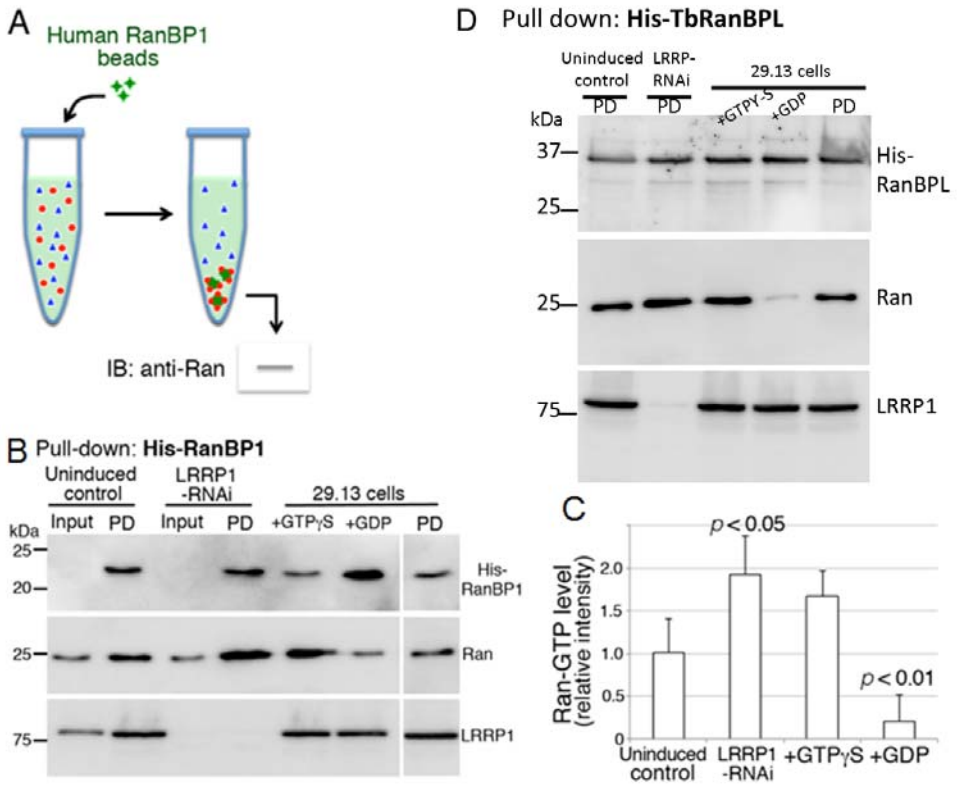

FIGURE 3.13 TbLRRP1 depletion inhibits RanGTP hydrolysis in *T. brucei* cell lysates. (A) The schematic depicts the rationale and experimental flow of the Ran Activation Assay (Cell Biolabs). (B) Ran activation was analyzed for both un-induced control and Ran-RNAi cell lysates, taking advantage of the highly specific binding of human RanBP1 to GTP-bound Ran, but not GDP-bound Ran. Control cell lysates loaded with GTPγS or GDP were used as control. (C) For quantitation, the relative intensity of the bands was read out for GTP-bound form. (D) His-tagged *T. brucei* RanBPL was used in place of human RanBP1 in the Ran activation assay. Control cell lysates preloaded with GTPγS or GDP were used as control. Input, 10% of total cell lysates; PD, pull-down products eluted from beads. Data shown represent averaged Ran-GTP levels (normalized against Ran-GTP pull-down from 29.13 cells) ± S.D., n=3 independent experiments. p values indicated for each condition were calculated by comparison to uninduced control cells.

3.6.3 Cellular distribution of GTP-bound Ran upon TbLRRP1 depletion

As shown earlier, RanBPL selectively binds to GTP-Ran, a conserved behavior of Ran binding proteins (Bischoff et al., 1995; Hayashi et al., 1995). This property was therefore used to monitor the level of GTP-bound Ran in *T. brucei,* in the presence or absence of endogenous TbLRRP1. TbLRRP1-RNAi cells were induced with tetracycline for 48 hours, fixed with PFA and permeablized by 0.25% Triton X-100. The cells were then incubated with purified His-RanBPL (1:200 diulation of 1mg/ml) in PBS containing 3% BSA for 1 hour at room temperature, allowing His-RanBPL to bind to GTP-Ran in situ. After extensive washes with PBS, the localization of His-RanBPL bound to cellular GTP-Ran was then monitored using anti-His antibody. As shown in Fig 3.14, in un-induced control cells, RanBPL localized primarily in the nucleus, suggesting enrichment of GTP-Ran in the nucleus, consistent with a nucleocytoplasmic Ran gradient observed in other eukaryotes. Upon TbLRRP1 depletion, His-RanBPL labelling became diffused throughout the cell, indicating a loss of Ran gradient in cells lacking TbLRRP1. This observation further supported TbLRRP1 was required for Ran regulation in *T. brucei*.

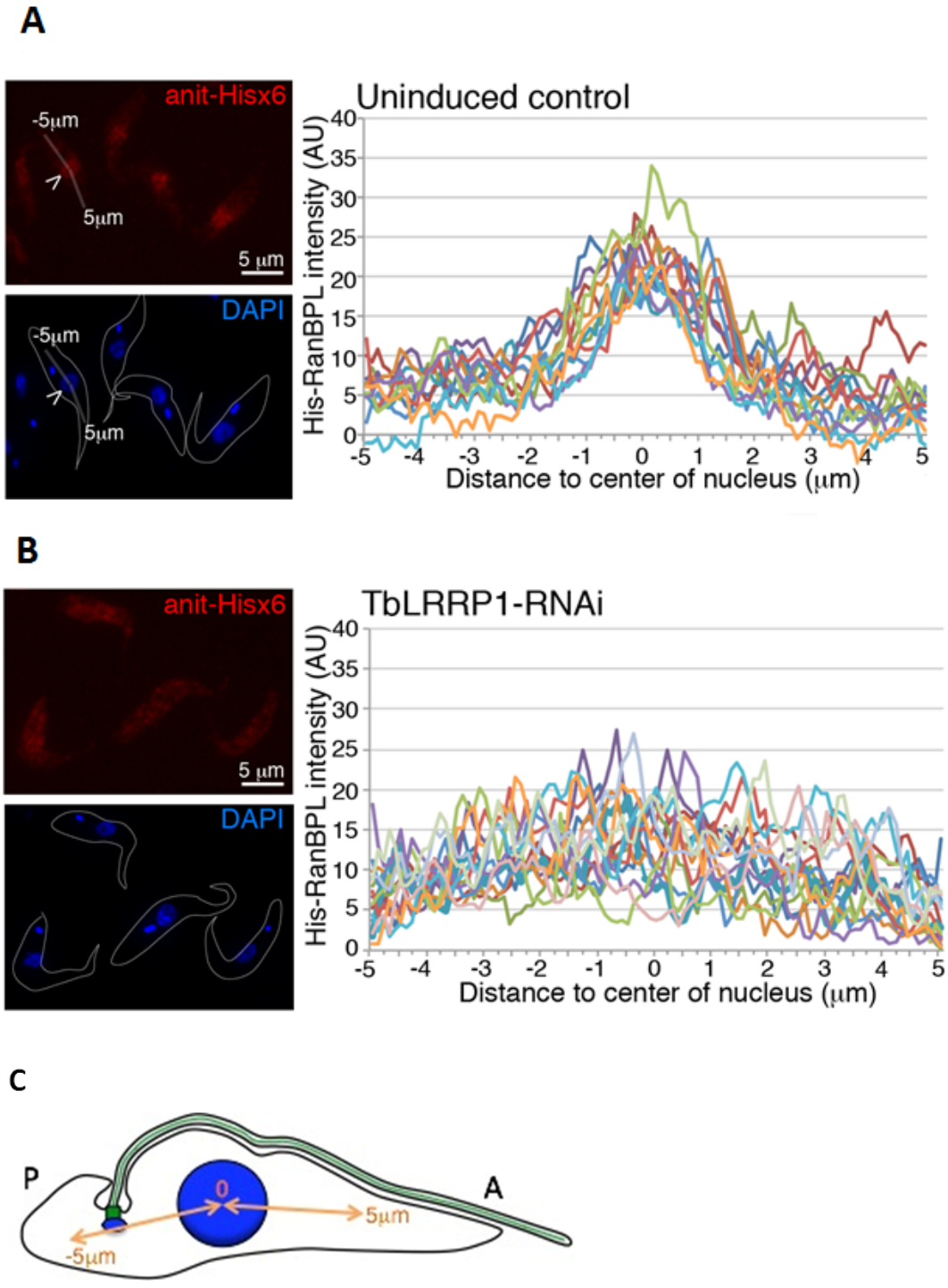

FIGURE 3. 14 Depletion of TbLRRP1 disrupts cellular Ran gradient. In situ labeling of GTP-Ran was performed using His-RanBPL in control (A) and TbLRRP1-RNAi cells (B). Scale bar=5μm. For quantitation, His-RanBPL intensity (AU) as indicated by anti-Hisx6 was measured along a 10 μm distance (5μm from the center of the single nucleus to the posterior and to the anterior side) for 12 cells each. P, posterior; A, anterior; 0, the center of the single nucleus (C).

CHAPTER 4 Discussion

TbLRRP1 is present exclusively on the bi-lobed structure (Zhou et al. 2010), which occupies a pivotal position at the proximal base of both the flagellum and the FAZ, and is tightly linked to the flagellar pocket collar (FPC) that constricts plasma membrane around the point of flagellum exit of the parasite body (Lacomble et al., 2009; Morriswood et al., 2009; Zhou et al., 2010; Shi et al., 2008; de Graffenried et al., 2008; Ikeda et al., 2012). In the procyclic cells, the bilobe is also closely associated with the single Golgi and ER exit site (He et al., 2005). Initially thought to be important for Golgi duplication and segregation, recent studies suggested that the bilobe may play a more fundamental role on the flagellum and flagellum associated structures. The exact function and the mechanism of the bilobe are yet to be unraveled.

4.1 The exclusive presence and the essential functions of TbLRRP1 make it a useful marker to study bilobe functions and mechanisms.

TbLRRP1, a 713-amino acid protein comprises of an LRR-containing domain in N-terminal region and a C-terminal coiled-coil region. It is essential for parasite survival. Depletion of TbLRRP1 resulted in new FAZ assembly but only moderately affected new flagellum biogenesis, resulting in kinetoplast division

and cell division defects. The duplication of bilobe and bilobe associated Golgi and FPC was also inhibited (Zhou et al., 2010). The exclusive presence of the TbLRRP1 on the bilobe was likely mediated by a 50aa coiled-coil region in the C-terminal half of TbLRRP1, which was sufficient and necessary for targeting YFP reporter to the bilobe. TbLRRP1 thus provides a specific marker for bilobe immunoisolation and proteomics, which revealed extensive bilobe association with other subcellular structures (Gheiratmand et al., in press).

The domain organization of TbLRRP1 however, provided little clue to its biological function. Vfl1 in Chlamydomonas and CLERC in humans both contain leucine-rich repeats and coiled-coils in similar organizations, and they have been found associated with centrosomes or basal bodies (Silflow et al., 2001; Muto et al., 2008). Deficiency in these proteins leads to flagellum biogenesis and mitotic spindle pole defects, though the exact mechanisms remained to be determined (Muto et al., 2010). However, the LRRs in Vfl1 and CLERC are distinct to the LRR in LRRP1. The latter belongs to the RI-like subfamily, which has been best characterized in ribonuclease inhibitors and yeast Rna1p, a RanGAP (Kobe et al., 2001; Bella et al., 2008; Hillig et al., 1999). The structure of Rna1p has been solved and shown to contain 11 Leucine- rich repeats, each of 28 to 37 residues, forming a crescent shape (Hillig et al., 1999). The interactions between Ran and RanGAP are mediated by 7 of the 11 LRRs (Vetter et al., 1999; Seewald et al., 2002; Seewald et al., 2003).

To understand the molecular mechanism of TbLRRP1 and to further investigate the function of the bi-lobe, we searched for *T. brucei* proteins interacting with the LRR domain or the coiled-coil domain, using yeast-two-hybrid screening. The most interesting binding candidate (encoded by Tb927.10.8650), containing a Ran-binding domain, was further characterized biochemically and cell biologically, leading to the serendipitous discovery of TbLRRP1 as a putative RanGAP.

4.2 RanGTPases

Ran is an abundant Ras-like small GTPase. It is initially characterized for its role in modulating nucleocytoplasmic transport of macromolecules across the nuclear envelope (Moore et al., 1994). Later studies also find Ran GTPases involved in mitotic spindle and nuclear envelope re-assembly during the cell cycle (Gruss et al., 2004; Ciciarello et al., 2007; Sazer and Dasso, 2000; Yudin and Fainzilber 2009). The proper functions of Ran rely on various Ran regulators, including RanGAP that induces GTP hydrolysis (Bischoff et al., 1994), RanGEF that triggers GDP to GTP exchanges (Bischoff et al., 1990; Nishitani et al., 1990), and also importins that control nuclear protein transport (Golrich et al., 1994; Mattaj et al., 1998). The combined action of RanGAP and RanGEF results in a nucleocytoplasmic RanGTP/RanGDP gradient, which is critical for the directional protein trafficking in and out of the nucleus (Avis et al., 1996; Stewart, 2007; Macara, 2001; Clark and Zhang 2008).

Recent years have seen exciting new discoveries of Ran functions in cilia protein trafficking (Obado and Rout, 2012; Hurd et al., 2011; Fan et al., 2011; Fan and Margolis, 2011; Li and Hu, 2011). Several studies showed that Ran and importin proteins are present in ciliary proteomes (Gherman et al., 2006; Liu et al., 2007; Pazour et al., 2005; Anderson et al. 2003). Consistent with this, importin-β1 was found to control the targeting of an apical polarity protein Crumbs3b to the centrosomal region (Fan et al., 2007), whereas importin-β2 was found to control the targeting of retinitis pigmentosa 2 into the cilia (Hurd et al., 2011, Fan et al., 2011). In an independent study, Ran and importin-β2 were found to regulate the ciliary entry of kinesin2 motor KIF17 in a similar manner of nuclear transport (Dishinger et al., 2010). The ciliary localization signal (CLS) identified in the KIF17 is similar to classic nuclear localization signals (NLSs) and is necessary and sufficient for cilium targeting. Like nuclear transport, high levels of RanGTP are present in the cilium and the ciliary-cytoplasmic gradient of Ran regulates the ciliary entry of kinesin motor KIF17 (Dishinger et al., 2010). Using an antibody that specifically detects Ran-GTP but not Ran-GDP (Lounsbury et al., 1996), Margolis group was able to recapitulate the above results in cilia from various cell types and tissues (Fan and Margolis 2011). Together, these studies provided the initial evidence demonstrating that RanGTP/ RanGDP gradient across the ciliary/cytoplasmic barrier regulates ciliary import.

Furthermore, similar to nuclear–cytoplasmic shuttling that is controlled by the NPC, a large multiprotein complex composed of multiple copies of 30 different

nucleoporin proteins that assemble into subcomplexes (Brohawn et al., 2009; D'Angelo and Hetzer, 2008) embedded in the double membrane of the nuclear envelope to form a pore-like structure (Fahrenkrog and Aebi, 2003), ciliary pores that act as a permeability barrier at the cilia base are proposed to control ciliary protein trafficking. Supporting this, several fluorescently-tagged nucleoporins including eGFP-NUP37 (outer ring nucleoporin), eGFP–NUP35 (inner ring nucleoporin), NUP93–eGFP3 (linker nucleoporin), and NUP62–eGFP3 (central phenylalanine–glycine (FG) nucleoporin) have been localized to ciliary base (Kee et al., 2012). eGFP–NUP214, a member of the cytoplasmic FG-containing nucleoporin and filament subcomplex, is localized in distinct puncta near basal bodies. However, as ciliary and nuclear import share several molecular and mechanistic features, how cargoes are distinguished from entering the cilium or the nucleus is unclear.

Compare to yeast and mammalian cells, the characterization of Ran in protozoan parasites lagged much behind. These studies were facilitated by the availability of the genomic databases. Ran has been found in many protozoan parasites including Giardia, apicomplexans and trypanosomatids (Chen et al., 1994; Frankel et al., 2008; Casanova et al., 2008). In *Toxoplasma gondii*, Ran was detected throughout the cell (Frankel et al., 2008). In *Leishmania major,* Ran was found to decorate a nuclear envelope 'collar' and to be closely associated with nuclear pore complexes (Casanova et al., 2008). Though lacking functional studies, the different cellular localization of Ran in these protists suggested potential

differences in transport machinery present in these organisms. For instance, Apicomplexans appear to lack several key nuclear transport proteins compared to other model organisms, or significant genetic drift has occurred in their nuclear transport proteins such that they are no longer recognized by BLAST searches. It is also suggested that these parasites encode minimal transport components that perform multiple, diverse functions (Frankel and Knoll, 2009). In *Leishmania major,* putative homologues of Ran partners such as RanBP1, CAS, and NTF2 were validated by colocalization studies with *Lmj*Ran to nuclear membrane punctates. BLAST analysis also identified one RanGAP candidate with a reasonable primary sequence similarity (34%) to yeast Rna1p. However, neither localisation nor biochemical studies, suggested any partnership of this protein with Ran (Casanova et al., 2008).

In *T. brucei*, a single homolog of Ran GTPase (rtb2) is encoded by Tb927.3.1120 (Field et al., 1995), whose amino acid sequence shows 83.5% identity and 92.2% similarity to *L. major* Ran, 68.9% identity and 78.5% similarity to yeast Ran. Stable expression of YFP-Ran or immunolabelling with an anti-Ran antibody resulted in distinct nuclear staining and weak cytoplasmic staining similar to yeast and human Ran but different to the more closely related *L. major* Ran (Casanova et al., 2008). Distinct nuclear localization of Ran was found throughout the cell cycle, as both the nuclear membrane and the NPCs remain intact during the closed mitosis. Also similar to the Ran GTPases found in yeast and mammals, *T.brucei* Ran T26N (a GDP-locked mutant) localized primarily in the nucleus, possibly due to its stable association with RCC1 (Lounsbury et al., 1996; Dasso et al., 1994). *T.*

brucei Ran G21V (a GTP-locked mutant), on the contrary, was present throughout the cell. These results indicated that *T. brucei* Ran behaved like an authentic Ran GTPase, similar to those found in yeast and mammal. Similar regulatory machineries, like RanGAPs and RanGEFs, may also be functioning in maintaining the Ran gradient in *T. brucei*.

4.3 Is TbLRRP1 a RanGAP?

Using yeast-two-hybrid screening, LRRP1 was found to interact with a previously uncharacterized Ran-binding protein RanBPL (encoded by Tb927.10.8650). Like RanBP1, *T. brucei* RanBPL bound to Ran in a GTP-dependent fashion. Further biochemical and cell biological characterization of TbLRRP1 interaction with *T. brucei* Ran and RanBPL supported the role of TbLRRP1 as a RanGAP. First, depletion of TbLRRP1 by RNAi led to disrupted Ran protein gradient and RanGTP/Ran-GDP gradient *in vivo*; second, TbLRRP1 was required for GTPase activity of Ran, as shown in *in vitro* assays; last but not least, TbLRRP1 formed a complex with RanBPL in a Ran-dependent fashion. However, direct biochemical analyses would be required to confirm the role of TbLRRP1 as a RanGAP. This has been challenging due to insolubility of TbLRRP1 when expressed in *E. coli*. The interaction between RanBPL and TbLRRP1 required the presence of Ran, similar to the Ran-RanGAP-RanBP1 interactions previously characterized (Seewald et al., 2002; Seewald et al., 2003). The identification of RanBPL as a

TbLRRP1-interacting partner was therefore a serendipitous finding, and their interaction in yeast was likely *via* endogenous yeast Ran.

In single-celled parasites, bioinformatic identification of RanGAP has not been straightforward due to sequence divergence. No RanGAP homologue has been found in apicomplexan parasites (Frankel et al., 2009). In *Leishmania spp*, a single, putative RanGAP homolog was identified by bioinformatic analyses but lacked functional characterization (Casanova et al., 2008). In the same study, a putative RanGAP that contained an RI-type LRR was also predicted for *T.brucei* (encoded by Tb927.7.1430). Neither the subcellular localization, nor RNAi knockdown of this putative RanGAP supported its association with Ran or its function as RanGAP. Our discovery of LRRP1 as a putative RanGAP with clear functions in Ran regulations thus provides the first characterization of a Ran-regulator in protozoan parasites.

4.4 LRR-containing proteins

TbLRRP1 is conserved only in trypanosomes. However, proteins with similar domain organization do exist in other eukaryotes and LRR-containing proteins are particularly abundant at basal bodies (Silflow et al., 2001; Muto et al., 2010). Many LRR-containing (LRRC) proteins have been implicated in ciliopathies. Serluca et al. (2009) reported the cloning and characterization of two alleles of

zebrafish *seahorse* (*sea*), sea^{tg238a} and sea^{fa20r}. *sea* encodes Lrrc61, a leucine-rich repeat-containing protein which is highly conserved in organisms that have motile cilia. They showed that the mentioned mutations in *lrrc6l* do not affect cilia structure, apical position of the basal body or the ability to interact with Disheveled, but result in severe cilia motility defects in the pronephros and neural tube that range from slow and disorganized cilia motility to immotile cilia. Thus, this study provided the first experimental evidence that *lrrc6l* is required for cilia motility *in vivo*.

Several ciliopathy-associated proteins localize to centriolar satellite (Lopes et al., 2011). To study the cellular and developmental consequences of disrupting centriolar satellites, Stowe et al. (2011) identified Cep72 as a new component of centriolar satellite that is required for the recruitment of the ciliopathy-associated protein Cep290 to the satellites. However, their analysis of human CEP72 revealed a related LRR-containing protein Lrrc36. CEP72 and Lrrc36 are part of a duplicated genome region in mammals and share a similar protein domain structure, consisting of conserved LRR domains at the N-terminus and a coiled-coil domain at the C-terminus. They showed the extensive co-localization of Cep72 with the centriolar satellite protein PCM1 (Pericentriolar material 1). In contrast, Lrrc36 localized to the pericentriolar material of the centrosome and did not overlap with PCM1.

In a forward genetic screen for mutations affecting ciliary motility, Rooijen et al., 2008, isolated zebrafish mutant *hu255H*. The mutation was found to disrupt an

ortholog of the uncharacterized highly conserved human SDS22-like leucine-rich repeat (LRR)-containing protein LRRC50 (16q24.1) and *Chlamydomonas* Oda7p. Zebrafish *lrrc50* is specifically expressed in all ciliated tissues. *lrrc50*^{hu255H} mutants develop pronephric cysts with an increased proliferative index, severely reduced brush border, and disorganized pronephric cilia manifesting impaired localized fluid flow consistent with ciliary dysfunction.

Mining of the *T. brucei* genome database revealed >50 LRR-containing proteins and >40 proteins contain RI-like type LRR (Table 4.1). Few of these LRR-containing proteins have been characterized (Morgan et al., 2004; Casanova et al., 2008; Zhou et al., 2010). TbLRTP displays significant similarity to LRTP, a testis specific protein of *Mus musculus* and *Homo sapiens* implicated in polycystic kidney disease (Xue et al., 2000). LRRs in TbLRTP are homologues of SDS22 subclass followed by a coiled-coil domain in C-terminal region. TbLRTP is found in association with the basal body that its expression is required for proliferation and completion of the cell cycle. Overexpression of TbLRTP suppresses basal body replication and new flagellum biogenesis. Depletion of the protein results in the biogenesis of additional ectopic basal bodies complete with an attached axoneme, paraflagellar rod, and FAZ associated microtubules (Morgan et al., 2005).

Though many of the *T. brucei* LRR-containing proteins may have other cellular functions (e.g. TbLRTP), it is possible that there are multiple RanGAPs present in *T. brucei* cells. TbLRRP1-RNAi depletion did not result in immediate mitotic

defects as have been observed in Ran-RNAi cells (our unpublished observations), also suggesting that other RanGAPs might be at work.

4.5 TbLRRP1 functions primarily on flagellum and associated structures

Not only divergent in primary sequence, the cellular localization of the RanGAP also varies in different organisms. Mammalian RanGAP targets to the NE during interphase and to the spindle and kinetochore during mitosis via a SUMOylated C-terminal domain (Meier et al., 2008). Plant RanGAP lacks the SUMOylated domain but contains a plant-specific N-terminal domain (WPP domain) that is responsible for RanGAP targeting to the nuclear rim (Rose et al., 2001). However, *Saccharomyces cerevisiae* RanGAP (Rna1P) is predominantly cytoplasmic without a significant concentration at the NE. Neither does it possess the SUMOylated domain. Unlike RanGAPs so far identified that is either on the nuclear envelope or in the cytosol (Meier et al., 2008; Rose et al., 2001; Frankel et al., 2009; Casanova et al., 2008), TbLRRP1 is a core cytoskeletal protein associated with the bilobe. The association is mostly resistance to detergent and high salt extractions (Zhou et al., 2010), though a small soluble pool (~30% of total TbLRRP1) was consistently observed (Ladan Gheiratmand, unpublished observation). Depletion of TbLRRP1 had no apparent effects on nuclear division or flagellum biogenesis, rather it inhibited the duplication of the bilobe and the assembly of the new FAZ, consequently inhibiting flagellum inheritance and

flagellum-driven cell motility and cell division (Zhou et al., 2010). Thus the primary function of TbLRRP1 is on the flagellum-associated structures such as the bilobe and the FAZ. FAZ is a complex structure required for flagellum attachment to the cell body. In addition to electron-dense protein filaments, the FAZ also contains a specialized set of four microtubules in close association with ER membrane (Sherwin and Gull, 1989a; Vickerman 1962; Vickerman 1969). During the cell cycle, FAZ assembles in co-ordination with flagellum (Kohl et al., 1999), driving cell growth, organelle segregation and cell division (LaCount et al., 2002; Morriswood et al., 2009; Shi et al., 2008; Zhou et al., 2010). Little, however, is known about the protein components and biogenesis of this structure.

Two proteins have been found associated with the FAZ filament. FAZ1, a repeat-containing protein is the first FAZ filament component and considered as a cytoskeletal structural protein on the cell body side of the FAZ filament. Knockdown of FAZ1 results in the assembly of a compromised FAZ and defects in flagellum attachment and cytokinesis in procyclic *T.brucei* (Kohl et al., 1999; Vaughan et al., 2008). CC2D is a new FAZ marker reported by Zhou et al. (2011). CC2D is also present on the basal bodies in procyclic *T.brucei.* Depletion of CC2D inhibits the elongation of new FAZ filament. Defective new FAZ assembly inhibits basal body segregation and subpellicular microtubule synthesis resulted in producing daughter cells with detached flagellum, shorter cell length and changed polarity (Zhou et al., 2011). Further studies of these proteins and characterization of other FAZ components will provide new insight into FAZ biogenesis and FAZ functions.

4.6 What does TbLRRP1 tell us about bilobe functions?

In addition to TbCentrin2, TbCentrin4, and TbMORN1, TbLRRP1 was the fourth protein identified by us to be stably associated with the bilobe. Initially thought to mediate Golgi/ER exit site biogenesis and inheritance, recent functional and morphological characterization of the bilobe structure suggested perhaps a more fundamental function of bilobe on flagellum and associated structures, most importantly the FAZ (Shi et al., 2008; de Graffenried et al., 2008; Zhou et al., 2010; Esson et al., 2012; Gheiratmand et al., in press).#

This study provided evidences supporting TbLRRP1 in Ran regulation. In light of recent findings highlighting the role of Ran-importin system in ciliary protein trafficking, we propose that the bilobe, strategically situated at the proximal base of the flagellum and FAZ and contained a putative RanGAP, may control protein trafficking into these structures. Whether or not the bilobe contains size exclusion pores requires further structural analyses. Interestingly, two centrin proteins TbCentrin2 and TbCentrin4 have both been found at the bilobe (He et al., 2005; Shi et al., 2008). In yeast, the single centrin CDC31 is also a nuclear pore complex component, interacting with SAC3 and regulating mRNA export from the nucleus (Fischer et al., 2004). In photoreceptor cells, centrins are located in the connecting cilium linking the light sensitive outer segment to the inner segment, perhaps functioning as a gatekeeper for light-induced translocation of

transducin through the connecting cilium (Gießl et al., 2006; Wolfrum and Salisbury, 1995; Wolfrum and Salisbury, 1998; wolfrum et al., 2002).

4.7 Future Works

Recent studies in mammalian cells have suggested a function of Ran in ciliary protein import, similar to its function in nuclear protein transport. Ran binding proteins including importins have also been found at the cilium base, and porous structures similar to nuclear pore complex were observed at the base of the flagellum/cilium, suggesting the mechanisms that regulate ciliary entry of soluble proteins may be mechanistically similar to those that regulate nuclear entry (Kee et al., 2012). How cargoes are distinguished from entering the cilium versus the nucleus is unclear. The complex molecular network at the base of the cilium also awaits further characterizations. The discovery of TbLRRP1, a bilobe associated putative RanGAP in *T. brucei,* opens up new means to study the function of Ran GTPase at flagellum/cilium.

It has long been established that the maintenance of RanGTPase gradient across the nuclear envelope relies on the combined action of RanGAP in the cytosol and RanGEF (RCC1) in the nucleus, allowing directional transport (Avis et al., 1996). Like nuclear transport, high levels of RanGTP are present in the cilium and the ciliary-cytoplasmic gradient of Ran regulates the ciliary entry of kinesin motor

KIF17 (Dishinger et al., 2010). In order to investigate the presence of a similar RanGTP/GDP gradient along the flagellum and FAZ, we need to explore other proteins involved in Ran regulation other than TbLRRP1. In particular, recent studies have identified a highly divergent ortholog of RCC1 that is critical for parasite pathogenesis (Frankel et al., 2007) and functions as a guanine nucleotide exchange factor (GEF) for Ran (Frankel and Knoll, 2009). In *Leshmania major* though none of the four putative homologues of RCC1 could induce any phenotype when tested by RNAi as is the case for Ran. These results could suggest that none of these proteins is the actual homologue of RCC1 (Casanova et al., 2008). However, in the most recent effort to identify *T.brucei* homologues of nuclear transport components (Yahya and Zuraina, 2010), RCC1 repeat were predicted using *in silico* approach. Thereby, it will be worth looking to study the function of RCC1 homologue in *T.brucei* particularly a flagellum/FAZ specific RanGEF.

Although TbLRRP1 is a bilobe resident protein, and was found as a core cytoskeletal component resistant to detergent and high salt extractions, it is not yet clear whether TbLRRP1 performs its RanGAP function at the bilobe. YFP-RanBPL was found throughout the cell and did not show enrichment on the bilobe at any time of the cell cycle, providing little clue to its functional site. *In vivo* evidence for Ran-RanBPL-TbLRRP1 interaction at the bilobe is needed. To examine if Ran and RanBPL might form complex with the bilobe LRRP1, a fluorescence resonance energy transfer (FRET) approach (Forster, 1948) can be used. For example, GFP-Ran and mRFP-TbLRRP1 will be co-expressed in *T.*

brucei and FRET responses will be measured at the bilobe region. Furthermore, a GFP bimolecular fluorescence complementation approach (Ghosh et al., 2000; Wilson et al., 2004; Magliery et al., 2004) can also be used. In this approach the GFP reporter protein is split into two non-fluorescent fragments, each fused to a bait and a pray protein, which are then co-expressed *in vivo*. Bait and pray interaction brings the GFP fragments together and reconstitutes green fluorescence. For example, NGFP-Ran and CGFP-LRRP will be co-expressed in *T.brucei.* If TbRan and TbLRRP interact with each other invivo, the GFP reporter will be reassembled and emit green fluorescence.

Once TbLRRP1 function as RanGAP on the bilobe is established by the above *in vivo* studies, further work will focus on characterization of nuclear-pore like function on the bilobe. Previous EM characterization of bilobe relied on detergent and salt-extraction of the flagellar complex (Esson et al., 2012), which removed most if not all soluble and membrane structures. In recent years, cryoelectron tomography has become a powerful tool to examine cellular structures in its native state (Koning et al., 2009). The technique involves the use of cell cultures frozen under vitreous conditions, which are cryosectioned into thin slices of 1μm. The specimen is then viewed using a stage which is capable of tilting at angles of $+70^{o}$ (Medalia et al., 2002; Beck et al., 2007; Robinson et al., 2007; Brandt et al., 2009; Nickell et al., 2009). This cutting-edge method has been explored in visualization of *T. brucei* flagellum, as well as other subcellular

structures (Höög et al., 2012; Koyfman et al., 2011; Hughes et al., 2012). Though an earlier tomographic study on chemically-preserved *T. brucei* did not find the bilobe (Lacomble et al., 2009), a re-examination of cryo-fixed *T. brucei* may allow better visualization of the structure.

A revisit of bilobe proteomes that were previously performed in our laboratory (Zhou et al., 2010; Gheiratmand et al., in press) revealed a putative nuclear protein, NUP-1 encoded by Tb927.2.4230 as well as some hypothetical proteins encoded by Tb927.7.6730, Tb927.10.14870, and Tb927.6.1180 which were localized to the nucleus. These were previously thought to be contaminants. A detailed characterization of these proteins, particularly their association with bilobe and their role in FAZ assembly, will be of potential interest.

T. brucei alone contains >40 LRR-containing proteins (Table 4.1). Whether or not they represent new basal body/bilobe proteins and if additional RanGAPs may be found in this subset of LRRC require further biochemical and cell biological assays as have been established in this study.

Table 4.1 List of LRR-containing proteins encoded by *T. brucei* genome.

Gene ID	Product description	Molecular weight	Protein length	Domain analysis	The presence of Coiled-coil region
Tb427.11.8950[1]	Leucine-rich repeat (TbLRRP1)	78962	713	RNI-like	485-531
Tb427.7.1430[2]	hypothetical protein, conserved, leucine-rich repeat protein (LRRP), putative	47760	448	RNI-like	Null
Tb427.3.4770[3]	hypothetical protein, conserved, leucine-rich repeat protein (LRRP), putative	44235	383	SDS22-like	Null
Tb427.01.3670	expression site-associated gene (ESAG) protein, putative	79389	713	N-t RING/U box; L-domain like; C-t RNI-like LRR	Null
Tb427.01.4180	hypothetical protein, conserved	81971	744	Near N-t RNI-like LRR;	636-685
Tb427.01.5030	leucine-rich repeat protein (LRRP), putative	80845	735	large L-domain like encompassing all most the entire protein	Null
Tb427.02.170	leucine-rich repeat protein (LRRP), putative	155867	1411	large RNI-like and L-domain like regions	43-81

[1] LRR-containing protein examined in the present study.
[2] LRR-containing protein studied by Casanova et al., 2008.
[3] LRR-containing protein studied by Morgan et al., 2005.

Tb427.03.1490	leucine-rich repeat protein (LRRP), putative	89965	816	large RNI-like and L-domain like regions	Null
Tb427.03.2950	hypothetical protein, conserved	83847	759	RNI-like	640-683
Tb427.05.590	protein phosphatase 1, regulatory subunit, putative	45774	403	Large L-domain like region	Null
Tb427.06.1550	hypothetical protein, conserved	38878	353	RNI-like	Null
Tb427.07.1430	hypothetical protein, conserved	47745	448	RNI-like	Null
Tb427.08.2120	hypothetical protein, conserved	39406	366	RNI-like	Null
Tb427.08.3790	paraflagellar rod component, putative (PFC2)	25120	223	L-domain like	Null
Tb427.10.1950	hypothetical protein, conserved	77142	711	RNI-like	Null
Tb427.10.9570	paraflagellar rod component, putative (PFC14)	118688	1082	RNI-like	Null
Tb427.10.10190	hypothetical protein, conserved	94628	846	L-domain like	Null
Tb427.10.14610	hypothetical protein, conserved	121431	1103	RNI-like	Null
Tb427tmp.53.0001	hypothetical protein	154805	1411	large L-domain like and RNI-like regions	48-80
Tb427tmp.02.2850	hypothetical protein, conserved	168350	1498	L-domain like and RNI-like	343-373
Tb427tmp.02.4230	hypothetical protein, conserved	95751	879	RNI-like	Null
Tb427.05.4400	hypothetical protein, conserved	47229	432	RNI-like	Null

Tb427tmp.02.2690	hypothetical protein, conserved	48616	440	RNI-like	Null
Tb427tmp.01.0680	leucine rich repeat (TbLRRP1)	78934	713	RNI-like	485-531
Tb427.03.580	leucine-rich repeat protein (LRRP), putative	64413	580	RNI-like	Null
Tb427.04.2460	kinatase, putative	142947	1286	tyr-kinase, L-like	Null
Tb427tmp.160.3410	leucine-rich repeat protein (LRRP), putative	52700	490	RNI-like	Null
Tb427tmp.46.0011	hypothetical protein, conserved	45573	415	RNI-like	Null
Tb427tmp.02.5220	dual specificity phopshatase, putative	46596	414	L-like and phosphotyrosine phosphatase	Null
Tb427.05.2270	hypothetical protein, conserved	53686	478	RNI-like	Null
Tb427.06.3560	hypothetical protein, conserved	168120	1483	L-like and IQ motif	1291-1323
Tb427.07.290	leucine-rich repeat protein (LRRP), putative	58725	537	RNI-like;RNI-like	Null
Tb427.07.6220	protein kinase, putative	60891	545	Protein Kinase; RNI-like	Null
Tb427.10.14460	hypothetical protein, conserved	111679	1012	RNI-like	Null
Tb427.07.2730	hypothetical protein, conserved	33928	307	RNI-like	Null
Tb427.07.5600	hypothetical protein, conserved	114581	1026	L-domain like	Null
Tb427tmp.02.1580	leucine-rich repeat protein (LRRP), putative	45150	408	L-domain like	Null

Tb427tmp.01.5250	hypothetical protein, conserved	37147	339	RNI-like	Null
Tb427tmp.01.8640	hypothetical protein, conserved	70716	628	RNI-like	Null
Tb427.04.2130	hypothetical protein, conserved	34819	318	RNI-like	Null
Tb427.05.3490	hypothetical protein, conserved	32747	304	RNI-like	Null
Tb427.07.250	hypothetical protein, conserved (ZC3H16)	64375	584	RNI-like	Null
Tb427tmp.160.1290	hypothetical protein, conserved	208794	1919	RNI-like	Null
Tb427tmp.211.0600	hypothetical protein, conserved	19933	180	RNI-like	Null
Tb427.10.820	hypothetical protein, conserved	37640	345	RNI-like	Null
Tb427.10.5980	hypothetical protein, conserved	46829	426	L-domain like	Null
Tb427tmp.02.3390	dynein light chain, putative	23960	210	L-domain like	Null
Tb427tmp.02.1420	hypothetical protein, conserved	74885	684	RNI-like (460-565)	Null
Tb427.06.410	hypothetical protein, conserved	94045	858	RNI-like (334-602, 505-850)	Null
Tb427.06.1160	hypothetical protein, conserved	80957	741	L-domain like (126-420)	Null
Tb427.07.7110	leucine-rich repeat protein (LRRP), putative	82459	743	RNI-like (170-437) and L-domain like (354-664)	112-151
Tb427.07.7180	leucine-rich repeat protein (LRRP), putative	71452	645	RNI-like (73-339) and L-domain like (256-566)	14-53
Tb427.08.6490	protein kinase, putative	119314	1078	Protein Kinase; L-domain like (714-859)	Null

Tb427.08.7950	hypothetical protein, conserved	191270	1747	RNI-like (1637-1742)	Null
Tb427tmp.02.1564	leucine-rich repeat protein (LRRP), putative	40115	370	RNI-like (41-368)	Null

BIBLIOGRAPHY

Absalon, S., L. Kohl, C. Branche, T. Blisnick, G. Toutirais, F. Rusconi, J. Cosson, M. Bonhivers, D. Robinson, and P. Bastin. 2007. Basal body positioning is controlled by flagellum formation in *Trypanosoma brucei*. *PloS one*. 2:e437.

Absalon, S., T.Blisnick, M. Bonhivers, L. Kohl, N. Cayet, G. Toutirais, J. Buisson, D. Robinson, and P. Bastin. 2008. Flagellum elongation is required for correct structure, orientation and function of the flagellar pocket in *Trypanosoma brucei*. *J.Cell Sci*. 121: 3704-3716.

Alastair G.B. S., J.R. Stevens, and J. Lukes. 2006. The evolution and the diversity of kinetoplastid flagellates. *TRENS in Parasitology*. 22(4):168-74.

Alsford, S., D.J. Turner, S.O. Obado, A. Sanchez-Flores, L. Glover, M. Berriman, C. Hertz-Fowler, and D. Horn. 2011. High-throughput phenotyping using parallel sequencing of RNA interference targets in the African trypanosome. *Genome research*. 21:915-924.

Andersen, JS., CJ. Wilkinson, T. Mayor, P. Mortensen, EA. Nigg, and M. Mann. 2003. Proteomic characterization of the human centrosome by protein correlation profiling. *Nature*, 426 (6966): 570-4.

Angelopoulos, E. 1970. Pellicular microtubules in the family Trypanosomatidae. *The Journal of protozoology*. 17:39-51.

Aslett, M., C. Aurrecoechea, M. Berriman, J. Brestelli, B.P. Brunk, M. Carrington, D.P. Depledge, S. Fischer, B. Gajria, X. Gao, M.J. Gardner, A. Gingle, G. Grant, O.S. Harb, M. Heiges, C. Hertz-Fowler, R. Houston, F. Innamorato, J. Iodice, J.C. Kissinger, E. Kraemer, W. Li, F.J. Logan, J.A. Miller, S. Mitra, P.J. Myler, V. Nayak, C. Pennington, I. Phan, D.F. Pinney, G. Ramasamy, M.B. Rogers, D.S. Roos, C. Ross, D. Sivam, D.F. Smith, G. Srinivasamoorthy, C.J. Stoeckert, Jr., S. Subramanian, R. Thibodeau, A. Tivey, C. Treatman, G. Velarde, and H. Wang. 2010. TriTrypDB: a functional genomic resource for the Trypanosomatidae. *Nucleic acids research*. 38:D457-462.

Archambault, V. and Glover, D. M. 2009. Polo-like kinases: conservation and divergence in their functions and regulation. *Nature Reviews Molecular Cell Biology* 10: 265-275.

Avis, JM., and RR. Clarke. 1996. Ran, a GTPase involved in nuclear processes: its regulators and effectors. *J. Cell. Sci.* 109 (10): 2423-7

Barr, F. A., H.H. Sillje, and E.A. Nigg. 2004. Polo-like kinases and the orchestration of cell division. *Nat Rev Mol Cell Biol* 5, 429-40.

Beck, M., V. Lucic, F. Förster, W. Baumeister and O. Medalia. 2007. Snapshots of nuclear pore complexes in action taken by cryoelectron tomography. *Nature* 449: 611-615.

Becker, J., F. Melchior, V. Gerke, F.R. Bischoff, H. Ponstingl, and A. Wittinghofer. 1995. RNA1 encodes a GTPase-activating protein specific for Gsp1p, the Ran/TC4 homologue of Saccharomyces cerevisiae. *J. Biol. Chem*. 270:11860-11865.

Bella, J., KL. Hindle, PA. McEwan, and SC. Lovell. 2008. The leucine-rich repeat srtucture. *Cell Mol Life Sci*, 65 (15): 2307-33

Berriman, M., E. Ghedin, C. Hertz-Fowler, G. Blandin, H. Renauld, D.C. Bartholomeu, N.J. Lennard, E. Caler, N.E. Hamlin, B. Haas, U. Bohme, L. Hannick, M.A. Aslett, J. Shallom, L. Marcello, L. Hou, B. Wickstead, U.C. Alsmark, C. Arrowsmith, R.J. Atkin, A.J. Barron, F. Bringaud, K. Brooks, M. Carrington, I. Cherevach, T.J. Chillingworth, C. Churcher, L.N. Clark, C.H. Corton, A. Cronin, R.M. Davies, J. Doggett, A. Djikeng, T. Feldblyum, M.C. Field, A. Fraser, I. Goodhead, Z. Hance, D. Harper, B.R. Harris, H. Hauser, J.

Hostetler, A. Ivens, K. Jagels, D. Johnson, J. Johnson, K. Jones, A.X. Kerhornou, H. Koo, N. Larke, S. Landfear, C. Larkin, V. Leech, A. Line, A. Lord, A. Macleod, P.J. Mooney, S. Moule, D.M. Martin, G.W. Morgan, K. Mungall, H. Norbertczak, D. Ormond, G. Pai, C.S. Peacock, J. Peterson, M.A. Quail, E. Rabbinowitsch, M.A. Rajandream, C. Reitter, S.L. Salzberg, M. Sanders, S. Schobel, S. Sharp, M. Simmonds, A.J. Simpson, L. Tallon, C.M. Turner, A. Tait, A.R. Tivey, S. Van Aken, D. Walker, D. Wanless, S. Wang, B. White, O. White, S. Whitehead, J. Woodward, J. Wortman, M.D. Adams, T.M. Embley, K. Gull, E. Ullu, J.D. Barry, A.H. Fairlamb, F. Opperdoes, B.G. Barrell, J.E. Donelson, N. Hall, C.M. Fraser, et al. 2005. The genome of the African trypanosome *Trypanosoma brucei*. Science (New York, N.Y.). 309:416-422.

Bischoff, FR., G.Maier, and G. Tilz.1990. A 47-kDa human nuclear protein recognized by antikinetochore autoimmune sera is homologous with the protein encoded by RCC1, a gene implicated in onset of chromosome condensation. *Proc Natl Acad Sci USA* 87:8617–8621

Bischoff, FR., C. Klebe, J. Kretschmer, A. Wittinghofer, and H. Ponstingl. 1994. RanGAP1 induces GTPase activity of nuclear-Ras related Ran. *Proc. Natl. Acad. Sci.USA*, 91: 2587-2591

Bischoff, FR., H. Krebber, E. Smirnova, W. Dong, and H. Ponstlingl. 1995. Co-activation of Ran-GTPase and inhibition of GTP dissociation by Ran-GTP binding protein RanBP1. *The EMBO Journal*. Vol 14 (4): 705-715.

Bos, JL., H. Rehmman and A. Wittinghofer. 2007. GEFs and GAPs: Critical Elements in the Control of Small G Proteins. *Cell*, 129 (5): 865-877.

Brandt, F., S.A. Etchells, J.O. Ortiz, A.H. Elcock, F.U. Hartl and W. Baumeister. 2009. The native 3D organization of bacterial polysomes. *Cell*, 136: 261-271.

Broadhead, R., Dawe, H. R., Farr, H., Griffiths, S., Hart, S. R., Portman, N., Shaw, M. K., Ginger, M. L., Gaskell, S. J., McKean, P. G. et al. 2006. Flagellar motility is required for the viability of the bloodstream trypanosome. *Nature* 440, 224-7.

Brohawn, S. G., J.R. Partridge, J. R. Whittle, and T.U. Schwartz. 2009. The nuclear pore complex has entered the atomic age. *Structure* 17**,** 1156–1168

Brun, R., J. Blum, F. Chappuis, and C. Burri. 2010. Human African trypanosomiasis. *Lancet*. 375:148-159.

Burkard, G., P., Judzi, and I., Roditi. 2011. Genome-wide RNAi screens in bloodstream forms Trypanosomesidentify drug transporters. *Molecular and Biochemical parasitology*. 175: 91-94.

Burkhard, P., Stetefeld, J. and Strelkov, S. V. (2001). Coiled coils: a highly versatile protein folding motif. *Trends Cell Biol* 11, 82-88.

Casanova, M., P. Portale, C. Blaineau, L. Crobu, P. Bastien, and M. Pages. 2008. Inhibition of active nuclear transport is an intrinsic trigger of programmed cell death in trypanosomatids. *Cell Death and Differentiation*. 15: 1910–1920.

Chen, LM., Y. Chern, SJ. Ong, and JH. Tai. 1994. Molecular cloning and characterization of a ras-related gene of ran/tc4/spi1 subfamily in *Giardia lamblia*. *J Biol Chem.* 24;269(25):17297-304.

Chen, H., E.R. Farkas, and W.W. Webb. 2008. In vivo applications of fluorescence correlation spectroscopy. *Methods in cell biology*, 89: 3-35.

Ciciarello M, R. Mangiacasale, and P. Lavia. 2007. "Spatial control of mitosis by the GTPase Ran". *Cell. Mol. Life Sci*. 64 (15): 1891–914.

Clarke, PR., and C. Zhang. 2008. Spatial and temporal coordination of mitosis by RanGTPase. *Nat Rev Mol Cell Biol.* 9 (6): 464-77.

Cross, G.A. 2001. African trypanosomes in the 21st century: what is their future in science and in health? *International journal for parasitology*. 31:427-433.

D'Angelo, M. A. and M.W. Hetzer. 2008. Structure, dynamics and function of nuclear pore complexes. *Trends Cell Bio*l. 18, 456–466.

Dasso, M., T. Seki, Y. Azuma, T. Ohba and T. Nishimoto, 1994. A mutant form of the Ran/TC4 protein disrupts nuclear function in *Xenopus laevis* egg extracts by inhibiting the RCC1 protein, a regulator of chromosome condensation. *EMBO J*. 13: 5732– 5744.

de Graffenried, C. L., Ho, H. H. and Warren, G. 2008. Polo-like kinase is required for Golgi and bilobe biogenesis in *Trypanosoma brucei*. *J Cell Biol* 181, 431-8.

Dishinger JF., HL. Kee, PM. Jenkins, S. Fan, TW. Hurd, JW. Hammond, YN. Truong, B. Margolis, JR. Martens, and KJ. Verhey. 2010. Ciliary entry of the kinesin-2 motor KIF17 is regulated by importin-beta2 and RanGTP. *Nat Cell Biol.*12(7):703-10.

Ehrenberg, M., and R. Rigler. 1974. Rotational brownian motion and fluorescence intensity fluctuations. *Chem Phys*, 4: 390–401.

Elson, E. L., and D. Magde. 1974. Fluorescence correlation spectroscopy I. Conceptual basis and theory. *Biopolymers*, 13: 1–27.

Esson, H. J., Morriswood, B., Yavuz, S., Vidilaseris, K., Dong, G. and Warren, G. 2012. Morphology of the trypanosome bilobe, a novel cytoskeletal structure. *Eukaryot Cell*.11 (6): 761-77.

Fahrenkrog, B., and U. Aebi. 2003. The nuclear pore complex: nucleocytoplasmic transport and beyond. *Nat. Rev. Mol. Cell biol*. 4:757-766

Fan, S., V. Fogg, Q. Wang, XW. Chen, CJ. Liu, and B. Margolis. 2007. A novel Crumbs3 isoform regulates cell division and ciliogenesis via importin beta interactions. *Journal of Cell Biology*. 178 (3): 378-98.

Fan, S., EL. Whiteman, TW. Hurd, JC. McIntyre, JF. Dishinger, CJ. Liu, RM. JR. Martens, KJ. Verhey, U. Sajjan, and B. Margolis. 2011. Induction of Ran GTP drives ciliogenesis. *Molecular biology of the cell.* 22 (23): 4539-4538.

Fan, S. and B. Margolis, 2011. The Ran importin system in cilia trafficking. *Organogenesis*. 7 (3): 147-53.

Fenn, K., and K.R. Matthews. 2007. The cell biology of *Trypanosoma brucei* differentiation. *Current opinion in microbiology*. 10:539-546.

Field MC., H. Field, JC. Boothroyd. 1995. A homologue of the nuclear GTPase ran/TC4 from *Trypanosoma brucei*. *Mol Biochem Parasitol*. 69: 131–134.

Fischer, T., S.R. Navarro, G. Pereira, A. Racz, E. Schiebel, and E. Hurt. 2004. Yeast centrin Cdc31is linked to the nuclear mRNA ezport machinery. *Nature Cell Biology*, 6(9): 840-8.

Frankel, M.B., D.G. Mordue, and L.J. Knoll. 2007. Discovery of parasite virulence genes reveals a unique regulator of chromosome condensation 1 ortholog critical for efficient nuclear trafficking. *Proc Natl Acad Sci USA* 104, 10181–10186.

Frankel, M.B., and L.J. Knoll. 2008. Functional analysis of key nuclear trafficking components reveals an atypical Ran network required for parasite pathogenesis. *Mol Microbiol*, 70:410– 420.

Frankel, MB., and JM. Knoll. 2009. The Ins and Outs of Nuclear Trafficking: Unusual Aspects in Apicomplexan Parasites. *DNA and cell biology*. 28(6): 277-284.

Frankel, MB., 2009. Characterization of a unique nuclear transport pathway required for virulence of the parasite,*Toxoplasma gondii*.

Förster,T. 1948. Intermolecular energy migration and fluorescence. *Annalen der Physik*, 437: 55–75.

Gheiratmand, L., A. Brasseur, Q. Zhou, C.Y. He. 2013. Biochemical characterization of the bi-lobe reveals a continious structural network linking the bi-lobe to other single-copied organelles in *Trypanosoma brucei*. *The journal of biological chemistry*, 288 (5): 3489- 3499.

Gherman, A., E. Davis, and N. Katsanis. N.2006. The ciliary proteome database: an integrated community resource for the genetic and functional dissection of cilia. *Nat Genet* 38, 961–962.

Giessl, A., P. Trojan, S. Rausch, A. Purvermuller, U. Wolfram. 2006. Centrins, gatekeepers for the light-dependent rtanslocation of transducin through the photoreceptor cell connecting cilium. *Vision Reseasrch*. 46 (27): 4509-2.

Golsteyn, RM., SJ. Schultz, J. Bartek, A. Ziemiecki, T. Ried, EA. Nigg. 1994. Cell cycle analysis and chromosomal localization of human Plk1, a putative homologue of the mitotic kinases Drosophila polo and Saccharomyces cerevisiae Cdc5. *Journal of cell science*. 107 (Pt 6):1509-17.

Golsteyn, RM., KE. Mundt, AM. Fry, and EA. Nigg. 1995. Cell cycle regulation of the activity and subcellular localization of Plk1, a human protein kinase implicated in mitotic spindle function. *Journal of cell biology*. 129(6):1617-28.

Görlich, D., S. Prehn, RA. Laskey, and E. Hartmann.1994. Isolation of a protein that is essential for the first step of nuclear protein import". *Cell*, 79 (5): 767–78

Ghosh, I., AD. Hamilton, L. Regan. 2000. Antiparallel leucine zipper directed protein reassembly: application to the green fluorscent protein. *J Am Chem Soc* 122: 56-58.

Gruss O.J., and I. Vernos. 2004. The machanism of spindle assembly. *J Cell Biol*. 27; 166(7): 949–955.

Gull, K. 1999. The cytoskeleton of trypanosomatid parasites. *Annual review of microbiology*. 53:629-655.

Hammarton, T.C., J. Clark, F. Douglas, M. Boshart, and J.C. Mottram. 2003. Stage-specific differences in cell cycle control in *Trypanosoma brucei* revealed by RNA interference of a mitotic cyclin. *The Journal of biological chemistry*. 278:22877-22886.

Hammarton, T. C., Kramer, S., Tetley, L., Boshart, M. and Mottram, J. C. 2007. *Trypanosoma brucei* Polo-like kinase is essential for basal body duplication, kDNA segregation and cytokinesis. *Molecular Microbiology* 65, 1229-1248.

Hayashi N., N. Yokoyama, T. Seki, Y. Azuma, T.Ohba, and N. Takeharu. RanBP1, a Ras-like nuclear G protein binding to Ran/TC4, inhibits RCC1 via Ran/TC4. *Molecular and General Genetics MGG*. 247 (6), pp 661-669

He, C. Y., Pypaert, M. and Warren, G. 2005. Golgi duplication in *Trypanosoma brucei* requires Centrin2. *Science,* 310: 1196-8.

Hillig RC., L. Renault, IR. Vetter, T. Drell, A. Wittinghofer, J. Becker. 1999. The crystal structure of rna1p: a new fold for a GTPase-activating protein. *Mol Cell*, 3:781-791.

Hengen, P.N. 1997. False positives from the yeast two-hybrid system. *Trends Biochem Sci*. 22:33-34.

Hoog, J.L., C.B. Marquis, J.R., Mcintosh, A. Hoenger, and K.Gull. 2012. Cryoelectron tomography and 3-D analysis of the intact flagellum in *Trypanosoma brucei*. *Journal of structural biology*, 178 (2): 189-198.

Hughes, LC., KS. Ralston, KL. Hill, and Z.H. Zhou. 2012. Three-dimentional structure of the trypanosome flagellum suggests that the paraflagellar rode functions as a biomechanical spring. *PLoS One*, 7 (1): 1-10.

Hurd, TW., S. Fan, and BL. Margolis. 2011. Localization of retinitis pigmentosa 2 to cilia is regulated by importin ß2. *Journal of Cell Science.* 124: 718-726.

Ikeda, K. N. and de Graffenried, C. L. 2012. Polo-like kinase is necessary for flagellum inheritance in *Trypanosoma brucei*. *J Cell Sci* 125, 3173-84.

Joseph, J. 2006. Ran at a glance. *J Cell Sci* 119: 3481-3484.

Kee, H.L., J.F. Dishinger, T.L. Blasius, C.J. Liu, B. Margolis, and K.J. Verhey. 2012. *Nature cell biology.* 14(4): 431-437

Keller GA, S. Krisans, SJ. Gould, JM. Sommer, CC. Wang , W. Schliebs, W. Kunau, S. Brody , S. Subramani. Evolutionary conservation of a microbody targeting signal that targets proteins to peroxisomes, glyoxysomes, and glycosomes. *J Cell Biol*. 114(5):893-904.

Kelly, S., J. Reed, S. Kramer, L. Ellis, H. Webb, J. Sunter, J. Salje, N. Marinsek, K. Gull, B. Wickstead, and M. Carrington. 2007. Functional genomics in *Trypanosoma brucei*: a collection of vectors for the expression of tagged proteins from endogenous and ectopic gene loci. *Molecular and biochemical parasitology*. 154:103-109.

Kobe, B. and Kajava, A. V. 2001. The leucine-rich repeat as a protein recognition motif. *Curr Opin Struct Biol* 11, 725-32.

Kohl, L., D. Robinson, and P. Bastin. 2003. Novel roles for the flagellum in cell morphogenesis and cytokinesis of trypanosomes. *The EMBO journal*. 22:5336-5346.

Kohl, L., T. Sherwin, and K. Gull. 1999. Assembly of the paraflagellar rod and the flagellum attachment zone complex during the *Trypanosoma brucei* cell cycle. *The Journal of eukaryotic microbiology*. 46:105-109.

Koning, R. I., and A. Koster. 2009. Cryo-electron tomography in biology and medicine. *Ann. Anat.* 191, 427-445.

Koyfman, A.Y., M.F. Schmid, L. Gheiratmand, CJ. Fu, H.A. Khant, D. Huang, C.Y. He, and W. Chiu. 2011. Structure of *Trypanosoma brucei* flagellum accounts for its bihelical motion.*PNAS,* 108 (27): 11105-11108.

Kumar, P. and Wang, C. C. 2006. Dissociation of Cytokinesis Initiation from Mitotic Control in a Eukaryote. *Eukaryotic Cell* 5, 92-102.

Lacomble, S., S. Vaughan, C. Gadelha, M.K. Morphew, M.K. Shaw, J.R. McIntosh, and K. Gull. 2009. Three-dimensional cellular architecture of the flagellar pocket and associated cytoskeleton in trypanosomes revealed by electron microscope tomography. *Journal of cell science*. 122:1081-1090.

Lacomble, S., S. Vaughan, C. Gadelha, M.K. Morphew, M.K. Shaw, J.R. McIntosh, and K. Gull. 2010. Basal body movements orchestrate membrane organelle division and cell morphogenesis in *Trypanosoma brucei*. *Journal of cell science*. 123:2884-2891.

LaCount, D. J., B. Barrett, and J.E., Donelson . 2002. *Trypanosoma brucei* FLA1 is required for flagellum attachment and cytokinesis. *J Biol Chem* 277, 17580-8.

Li, Z., and C.C. Wang. 2003. A PHO80-like cyclin and a B-type cyclin control the cell cycle of the procyclic form of *Trypanosoma brucei*. *The Journal of biological chemistry*. 278:20652-20658.

Li, Y., and J.Hu. 2011. Small GTPases and cilia. *Protein Cell*. 2 (1): 13-25.

Liu, Q., G. Tan, N. Levenkova, T. Li, E. Pugh, E.N. Jr, J.J. Rux, D.W. Speicher, and E.A. Pierce, 2007. The proteome of the mouse photoreceptor sensory cilium complex. *Mol Cell Proteomics* 6, 1299–1317.

Lopes, C.A., S.L. Prosser, L. Romio, R.A. Hirst, C. O'Callaghan, A.S. Woolf, and A.M.,Fry. 2011. Centriolar satellites are assembly points for proteins implicated in human ciliopathies, including oral-facial-digital syndrome 1. *J Cell Sci* 124: 600-612.

Lounsbury, K. M., S. A. Richards, R. R. Perlungher and I. G. Macara. 1996. Ran binding domains promote the interaction of Ran with p97/b-karyopherin, linking the docking and translocation steps of nuclear import. *J. Biol. Chem.* 271: 2357–2360.

Macara, IG. 2001. Transport into and out of the nucleus. *Microbiol Mol Biol Rev.*65 (4): 570-594.

Magde, D., E.L., Elson, and W.W. Webb. 1972. Thermodynamic fluctuations in a reacting system: Measurement by fluorescence correlation spectroscopy. *Phys Rev Lett*, 29: 705–708.

Magde, D., E.L. Elson, and W.W. Webb. 1974. Fluorescence correlation spectroscopy II. An experimental realization. *Biopolymers*, 13, 29–61.

Magliery, TJ., C.GM. Wilson, W. Pan, D. Mishler, I. Ghosh , AD. Hamilton, L. Regan. 2005. Detecting protein-protein interactions with a GFP-fragment reassembly trap: scope and mechanism. *J Am Chem Soc*, 127: 146-157

Marchetti, M., C. Tschundi, and H. Kwon. 2000. Import of proteins into the trypanosome nucleus and their distribution at karyokinesis. *Journal of cell science*. 113:899-906.

Mattaj, IW., and L. Englmeier. 1998. Nucleocytoplasmic transport: the soluble phase. *Annu. Rev. Biochem*. 67: 265–306.

Matthews, K.R. 2005. The developmental cell biology of *Trypanosoma brucei*. *Journal of cell science*. 118:283-290.

McDonnell, A.V., T. Jiang, A.E. Keating, and B. Berger. 2006. Paircoil2: Improved prediction of coiled coils from sequence. *Bioinformatics*, 22(3): 356-358

Medalia, O., I. Weber, A.S. Frangakis, D. Nicastro, G. Gerisch and W. Baumeister. 2002. Macromolecular Architecture in Eukaryotic Cells Visualized by Cryoelecton Tomography. *Science*, 298: 1209-1213.

Meier I., and J. Brkljacic, 2009. The nuclear pore and plant development. *Current opinion in plant biology.*12 (1): 85-97.

Meissner, M., C. Agop-Nersesian, and W.J. Sullivan, Jr. 2007. Molecular tools for analysis of gene function in parasitic microorganisms. *Applied microbiology and biotechnology*. 75:963-975.

Moore MS., and G. Blobel. 1994. A G protein involved in nucleocytoplasmic transport: the role of Ran. *Trends Biochem. Sci*. 19 (5): 211–216.

Morgan, G.W., W.D. Paul, S. Vaughen, D. Goulding, T.R. Jefrries, D.F. Smith, K. Gull and M.C. Field. 2004. An Evolutionarily Conserved Coiled-Coil Protein Implicated in Polycystic Kidney Disease Is Involved in Basal Body Duplication and Flagellar Biogenesis in *Trypanosoma brucei* . *Molecular and cellular biology.*25 (9): 3374-3383

Morris, J.C., Z. Wang, M.E. Drew, and P.T. Englund. 2002. Glycolysis modulates trypanosome glycoprotein expression as revealed by an RNAi library. *The EMBO journal*. 21:4429-4438.

Morriswood, B., C.Y. He, M. Sealey-Cardona, J. Yelinek, M. Pypaert, and G. Warren. 2009. The bilobe structure of *Trypanosoma brucei* contains a MORN-repeat protein. *Molecular and biochemical parasitology*. 167:95-103.

Motyka, S.A., and P.T. Englund. 2004. RNA interference for analysis of gene function in trypanosomatids. *Current opinion in microbiology*. 7:362-368.

Murrell, J. R. and D. D. Hunter, 1999. An olfactory sensory neuron line, odora, properly targets olfactory proteins and responds to odorants. *J. Neurosci.* 19, 8260–8270 (1999).

Muto, Y., T. Yoshioka, M. Kimura, M. Matsunami, H. Saya, and Y. Okano. 2010. An evolutionary conserved leucine-rich repeat protein CLERC is a centrosomal protein required for spindle pole integrity. *Cell cycle*. 7:17, 2738-2748.

Nickell, S., F. Beck, S.H.W. Scheres, A. Korinek, F. Förster, K. Lasker, O. Mihalache, N. Sun, I. Nagy, A. Sali, J.M. Plitzko, J.M. Carazo, M. Mann and W. Baumeister. 2009. Insights into the molecular architecture of the 26S proteasome. *PNAS*, 106: 11943-11947.

Nishitani, H., H. Kobayashi, and M. Ohtsubo. 1990. Cloning of Xenopus RCC1 cDNA, a homolog of the human RCC1 gene: complementation of tsBN2 mutation and identification of the product. *J Biochem (Tokyo)*, 107:228–235.

Obado, SO, and MP. Rout. 2012. Ciliary and nuclear transport: different places, similar routes? *Developmental Cell.* 22(4): 693-4.

Ogbadoyi, E., K. Ersfeld, D. Robinson, T. Sherwin, and K. Gull. 2000. Architecture of the *Trypanosoma brucei* nucleus during interphase and mitosis. *Chromosoma*. 108:501-513.

Ogbadoyi, E.O., D.R. Robinson, and K. Gull. 2003. A high-order trans-membrane structural linkage is responsible for mitochondrial genome positioning and segregation by flagellar basal bodies in trypanosomes. *Molecular biology of the cell*. 14:1769-1779.

Pazour, GJ., N. Agrin, J. Leszyk, and GB. Witman. 2005. Proteomic analysis of a eukaryotic cilium. *Journal of Cell Biology*. 170 (1): 103-13

Ploubidou, A., D.R. Robinson, R.C. Docherty, E.O. Ogbadoyi, and K. Gull. 1999. Evidence for novel cell cycle checkpoints in trypanosomes: kinetoplast segregation and cytokinesis in the absence of mitosis. *Journal of cell science*. 112 (Pt 24):4641-4650.

Peters, U., J. Cherian, J.H. Kim, B.H. Kwok, and T.M. Kapur. 2006. Probing cell-division phenotype space and Polo-like kinase function using small molecules. *Nature Chemical Biology* **2**, 618 - 626

Redmond, S., J. Vadivelu, and M.C. Field. 2003. RNAit: an automated web-based tool for the selection of RNAi targets in *Trypanosoma brucei*. *Molecular and biochemical parasitology*. 128:115-118.

Robinson, D.R., and K. Gull. 1991. Basal body movements as a mechanism for mitochondrial genome segregation in the trypanosome cell cycle. *Nature*. 352:731-733.

Robinson, D.R., T. Sherwin, A. Ploubidou, E.H. Byard, and K. Gull. 1995. Microtubule polarity and dynamics in the control of organelle positioning, segregation, and cytokinesis in the trypanosome cell cycle. *The Journal of cell biology*. 128:1163-1172.

Robinson, C.V., A.Sali and W. Baumeister. 2007. The molecular sociology of the cell. *Nature*, 450: 973-982.

Roditi, I., and M.J. Lehane. 2008. Interactions between trypanosomes and tsetse flies. *Current opinion in microbiology*. 11:345-351.

Rooijen, E.V., R.H. GIles, E.E. Voest, C.V. Rooijen, S.S. Merker, and F.J. van Eeden. 2008. *J Am Soc Nephrol*, 19: 1128-1138.

Rosario, V. 1981. Cloning of naturally occurring mixed infections of malaria parasites. *Science (New York, N.Y.)*. 212:1037-1038.

Rose, A. and I. Meier, 2001. A domain unique to plant RanGAP is responsible for its targeting to the plant nuclear rim. *PNAS*. 98 (26): 15377-15382.

Ruben, L., C. Egwuagu, and C.L. Patton. 1983. African trypanosomes contain calmodulin which is distinct from host calmodulin. *Biochimica et biophysica acta*. 758:104-113.

Scott, V., T. Sherwin, and K. Gull. 1997. gamma-tubulin in trypanosomes: molecular characterisation and localisation to multiple and diverse microtubule organising centres. *Journal of cell science*. 110 (Pt 2):157-168.

Seewald M.J., C. Korner, A. Wittinghofer, and Vetter I.R. 2002. RanGAP mediates GTP hydrolysis without an arginine finger. *Nature*. 415: 662-6.

Seewald, M.J., A. Kraemer, M. Farkasovsky, C. Kornar, A. Wittinghofer, and IR. Vetter. 2003. Biochemical Characterization of the Ran-RanBP1-RanGAP System: Are RanBP Proteins and the Acidic Tail of RanGAP Required for the Ran-RanGAP GTPase Reaction?*Mol Cell Biol*. 23 (22): 8124-8136.

Serluca, F.C., B. Xu, N. Okabe, K.Baker, S.Y. Lin, J.S. Brown, D.J. Konieczkowski, K.M. Jaffe, J.M. Bradner, M.C. Fishman and R.D. Burdine. 2009. Mutation in zebrafish Leucine-rich repeat-containing six-like affect cilia motility and result in pronephric cysts, but have variable effects on left-right patterning. *Development*, 136 (10): 1621-1631.

Sezar, S., and M. Dasso. 2000. The ran decathlon: multiple roles of Ran. *Journal of Cell Science*, 113 (7): 1111-1118.

Sherwin, T., and K. Gull. 1989a. The cell division cycle of *Trypanosoma brucei brucei*: timing of event markers and cytoskeletal modulations. *Philosophical transactions of the Royal Society of London. Series B, Biological sciences*. 323:573-588.

Sherwin, T., and K. Gull. 1989b. Visualization of detyrosination along single microtubules reveals novel mechanisms of assembly during cytoskeletal duplication in trypanosomes. *Cell*. 57:211-221.

Shi, J., Franklin, J. B., Yelinek, J. T., Ebersberger, I., Warren, G. and He, C. Y. 2008. Centrin4 coordinates cell and nuclear division in *T. brucei*. *J Cell Sci* 121, 3062-70.

Shi, H., A. Djikeng, T. Mark, E. Wirtz, C. Tschudi, and E. Ullu. 2000. Genetic interference in *Trypanosoma brucei* by heritable and inducible double-stranded RNA. *RNA (New York, N.Y.)*. 6:1069-1076.

Silflow, CD., M. LaVoice, MW. Tam, S.Tousey, M. Sanders, W. Wu, M. Borodovsky, and PA. Lefebvre. 2001. The Vfl1 protein in *Chlamydomonas* localizes in a rotationally asymmetric pattern at the distal ends of the basal bodies. *The Journal of Cell Biology*. 153 (1): 63-74.

Simarro, P.P., J. Jannin, and P. Cattand. 2008. Eliminating human African trypanosomiasis: where do we stand and what comes next? *PLoS medicine*. 5:e55.

Stewart, M. 2007. Molecular mechanism of the nuclear protein import cycle. *Nat Rev Mol Cell Biol* 8: 195–208.

Stowe, T.R., C.J. Wilkinson, A. Iqbal, and T. stearns. 2011. The centriolar satellite proteins Cep72 and Cep290 interact and are required for recruitment of BBS proteins to the cilium. *Molecular biology of the cell*, 23 (17): 3322-3335.

Thompson, N. L. 2002. Fluorescence correlation spectroscopy. *Topics in Fluorescence Spectroscopy Techniques*, 1: 337-378.

Yahya, M., and F. Zuraina. 2010. *International conference on science and social research*, December 5-7. Kuala lumpur, Malaysia.

Yudin, D., and M. Fainzilber. 2009. Ran on tracks--cytoplasmic roles for a nuclear regulator. *Journal of Cell Science*. 122:587-593.

Vassella, E., B. Reuner, B. Yutzy, and M. Boshart. 1997. Differentiation of African trypanosomes is controlled by a density sensing mechanism which signals cell cycle arrest via the cAMP pathway. *Journal of cell science*. 110 (Pt 21): 2661-2671.

Vaughan, S., L. Kohl, I. Ngai, R.J. Wheeler, and K. Gull. 2008. A repetitive protein essential for the flagellum attachment zone filament structure and function in *Trypanosoma brucei*. *Protist*. 159:127-136.

Vetter, IR., C. Nowak, T. Nishimoto, J. Kuhlmann, and A. Wittinghofer. 1999. Structure of a Ran-binding domain complexed with Ran bound to GTP analouge; implications for nuclear transport. *Nature*, 398:39-46.

Vickerman, K. 1962. Patterns of cellular organization in *Limax amoeba*. An electron microscope study. *Experimental cell research.* 26: 497-519.

Vickerman, K. 1969. On the surface coat and flagellar adhesion in trypanosomes. *Journal of cell science* 5: 163-93.

Vickerman, K., L. Tetley, K.A. Hendry, and C.M. Turner. 1988. Biology of African trypanosomes in the tsetse fly. *Biology of the cell / under the auspices of the European Cell Biology Organization*. 64:109-119.

Wilson, C.GM., T.J. Magliery, and L. Regan. 2004. Detecting protein-protein interactions with GFP-fragment reassembly. *Nature Methods*, 1 (3): 255-262.

Wirtz, E., S. Leal, C. Ochatt, and G.A. Cross. 1999. A tightly regulated inducible expression system for conditional gene knock-outs and dominant-negative genetics in *Trypanosoma brucei*. *Molecular and biochemical parasitology*. 99:89-101.

Wolfrum, U., and J.L. Salisbury, 1995. Centrin: a new Ca-binding protein and a noval component of the connecting cilium of photoreceptors in mammals and man. *Invest. Ophthalmol. Vis. Sci*. 36, 2379 (AbstractBook).

Wolfrum, U., and J.L. Salisbury, 1998. Expression of centrin isoforms in the mammalian retina. *Exp. Cell Res*. 242, 10–17.

Wolfrum, U., A. Giessl, A. Pulvermu¨ ller, 2002. Centrins, a novel group of Ca2+-binding proteins in vertebrate photoreceptor cells. *Adv. Exp. Med. Biol*. 514: 155–178.

Xue, J. C., and E. Goldberg. 2000. Identification of a novel testis-specific leucine-rich protein in humans and mice. *Biol. Reprod*. 62:1278–1284.

Zhang Y, MSc thesis 2012. Understanding the molecular mechanism of centrins in *Trypanosoma brucei*. 125 pages.

Zhou, Q., Gheiratmand, L., Chen, Y., Lim, T. K., Zhang, J., Li, S., Xia, N., Liu, B., Lin, Q. and He, C. Y. 2010. A comparative proteomic analysis reveals a new bi-lobe protein required for bi-lobe duplication and cell division in *Trypanosoma brucei*. *PLoS One* 5, e9660.

Zhou, Q., B. Liu, Y. Sun, and C.Y. He. 2011. A coiled-coil- and C2-domain-containing protein is required for FAZ assembly and cell morphology in *Trypanosoma brucei. Journal of cell science*. 124:3848-3858.